Copyright Warning & Restrictions

The copyright law of the United States (Title 17, United States Code) governs the making of photocopies or other reproductions of copyrighted material.

Under certain conditions specified in the law, libraries and archives are authorized to furnish a photocopy or other reproduction. One of these specified conditions is that the photocopy or reproduction is not to be "used for any purpose other than private study, scholarship, or research." If a, user makes a request for, or later uses, a photocopy or reproduction for purposes in excess of "fair use" that user may be liable for copyright infringement,

This institution reserves the right to refuse to accept a copying order if, in its judgment, fulfillment of the order would involve violation of copyright law.

Please Note: The author retains the copyright while the New Jersey Institute of Technology reserves the right to distribute this thesis or dissertation

Printing note: If you do not wish to print this page, then select "Pages from: first page # to: last page #" on the print dialog screen

ABSTRACT

A MULTIMODAL INVESTIGATION IN EYE MOVEMENTS

by

Raj Jaswal

While functional magnetic resonance imaging (fMRI) has identified which regions of interest (ROIs) are functionally active during a vergence movement (inward or outward eye rotation), task-modulated coactivation between ROIs is less understood. This study tests the following hypotheses: (1) significant task-modulated coactivation would be observed between the frontal eye fields (FEFs), the posterior parietal cortex (PPC), and the cerebellar vermis (CV); (2) significantly more functional activity and task-modulated coactivation would be observed in binocularly normal controls (BNCs) compared with convergence insufficiency (CI) subjects; and (3) after vergence training, the functional activity and task-modulated coactivation would increase in CIs compared with their baseline measurements. A block design of sustained fixation versus vergence eye movements stimulates activity in the FEFs, PPC, and CV. fMRI data from four CI subjects before and after vergence training are compared with seven BNCs. Functional activity is assessed using the blood oxygenation level dependent (BOLD) percent signal change. Task-modulated coactivation is assessed using an ROI-based task modulated coactivation analysis that reveals significant correlation between ROIs.

A MULTIMODAL INVESTIGATION IN EYE MOVEMENTS

by
Raj Jaswal

A Dissertation
Submitted to the Faculty of
New Jersey Institute of Technology
And Rutgers Biomedical and Health Sciences
in Partial Fulfillment of the Requirements for the Degree of
Doctor of Philosophy in Biomedical Engineering

Department of Biomedical Engineering

August 2016

.

APPROVAL PAGE

A MULTIMODAL INVESTIGATION IN EYE MOVEMENTS

Raj Jaswal

Dr. Tara L. Alvarez, Dissertation Advisor Professor of Biomedical Engineering, NJIT	Date
Dr. Bharat B. Biswal, Dissertation Co-Advisor Professor of Biomedical Engineering, NJIT	Date
Dr. Mitchell Scheiman , Committee Member Dean of Research, Salus University	Date
Dr. Kevin Pang, Committee Member Professor of Neuroscience, Rutgers New Jersey Medical School	Date
Dr. Eugene Tunik, Committee Member Professor of Neuroscience, Rutgers New Jersey Medical School	Date

BIOGRAPHICAL SKETCH

Author: Raj Jaswal

Degree: Doctor of Philosophy

Date: August 2016

Undergraduate and Graduate Education:

- Doctor of Philosophy in Biomedical Engineering,
  New Jersey Institute of Technology, Newark, NJ, 2016

- Master of Science in Biomedical Engineering,
  New Jersey Institute of Technology, Newark, NJ, 2009

- Master of Science in Electrical Engineering,
  New Jersey Institute of Technology, Newark, NJ, 2005

- Bachelor of Science in Electrical and Computer Engineering,
  Rutgers University, Piscataway, NJ, 2003

Major: Biomedical Engineering

Presentations and Publications:

Jaswal, R., Gohel, S., Biswal, B. B., & Alvarez, T. L. (2014). Task-modulated coactivation of vergence neural substrates. Brain Connectivity.

Alvarez, T. L., Jaswal, R., Gohel, S., & Biswal, B. B. (2014). Functional activity within the frontal eye fields, posterior parietal cortex, and cerebellar vermis significantly correlates to symmetrical vergence peak velocity: an ROI-based, fMRI study of vergence training. Frontiers in Integrative Neuroscience, 8, 50.

Jaswal, R., Alvarez, T. L., Gohel, Suril, & Biswal, B. B. (2014). Functional connectivity of vergence neural substrates. In Bioengineering, Proceedings of the Northeast Conference, Boston, MA.

Jaswal, R. and Alvarez, T. L. (2014). Stereoscopic vision and its asymmetrical underpinnings: A study in vergence measures. In Bioengineering, Proceedings of the Northeast Conference, Boston, MA.

Alkan, Y., Alvarez, T. L., Kim, E., Jaswal, R., Biswal, B. B., Gohel, S., & Vicci, V. R. (2009). Functional MRI as a tool to quantify cortical changes from vision rehabilitation. In Proceedings - International Conference on Tools with Artificial Intelligence, ICTAI (pp. 762-765), Newark, NJ.

Alvarez, T. L., Alkan, Y., Kim, E., Jaswal, R., Ludlam, D., Moinot, P., Vicci, V. R. (2009). Neuroplasticity in vision dysfunction. In 2009 4th International IEEE/EMBS Conference on Neural Engineering, NER (pp. 249-252).

Jaswal, R., Alvarez, T. L., Alkan, Y., Kim, E., & Biswal, B. B. (2009). The cerebral vascular enhancement effect in establishing diffusion tensor imaging protocols. In Proceedings - International Conference on Tools with Artificial Intelligence, ICTAI (pp. 771-775), Newark, NJ.

Kim, E. H., Alkan, Y., Jaswal, R., Ludlam, D., Biswal, B. B., Vicci, V. R., & Alvarez, T. L. (2009). ICA decomposition of vergence dynamics in convergence insufficiency patients. In Bioengineering, Proceedings of the Northeast Conference, New York, NY.

For wisdom is more precious than rubies, and nothing you desire can compare with her.

ACKNOWLEDGMENT

I would like to give my sincere appreciation to my advisor, Dr. Tara L. Alvarez. It is with her help and guidance that I was able to complete the Ph.D. dissertation.

I would also like to thank my co-advisor, Dr. Bharat B. Biswal who has provided me with the guidance I needed to prepare for my dissertation projects.

My sincerest thanks and gratitude goes to my committee members, Dr. Mitchell Scheiman, Dr. Eugene Tunik and Dr. Kevin Pang for making the time to advise me and provide constructive feedback as I prepared my dissertation.

I would like to thank all members of VNEL, past and current, for helping me get to this point.

A special thank you goes to Dr. Suril Gohel. With his help I was able to pick up the subtleties and nuances of fMRI image processing and made data interpretation more meaningful.

Thank you to the Bajaj family for their love and support.

Thank you to my family for being there for me, through the good days and especially through the tough ones. I have no idea how we made it through. Thank you to my mother, father, and brother.

And to Reem, I would never have been able to complete this journey without your strength and support. You set the framework for my progress.

TABLE OF CONTENTS

TABLE OF CONTENTS
(Continued)

LIST OF FIGURES

LIST OF FIGURES
(Continued)

Figure **Page**

CHAPTER 1

INTRODUCTION

1.1 Mission Statement

The Vision and Neural Engineering Laboratory (VNEL) at New Jersey Institute of Technology, Newark, NJ) mainly focuses its resources investigating how motor learning and adaptation together form the ability to modify a system, which is critical to survival. Our society is evolving and becoming more dependent on small mobile devices, which cause visual stress. Once adaptation is better understood, new therapies can be engineered to help those with vision dysfunctions and complaints, serving to improve quality of life and activities of daily living. The VNEL mission is to take the necessary first steps in understanding the underlying neurophysiology of oculomotor adaptation and to create translational research that will directly facilitate clinical care for those with oculomotor dysfunctions.

1.2 Background Information

The human visual system is designed to operate with a particular range of the electromagnetic spectrum, or light. Once light strikes the retina, the complex yet elegant task of visual processing begins that allows us to dynamically render the world as we see it. To understand visual processing, it is necessary to analyze visual patterns; what they consist of, and how they form (before they ever reach an eye). With information about the characteristics of visual patterns comes an understanding of how vision is constructed in the brain.

The eyes have been studied in great detail and we are still learning many characteristics of the eye with relation to each other. Late 19th and early 20th century investigations in eye movements (Buswell 1935, Huey 1898, Orschansky 1899) that sought to reliably measure and track eye positions have helped pioneer the field of vision research. Since then, many areas of interest have evolved, ranging from modeling oculomotor control systems (Semmlow et al. 1986, Hung et al. 2002, Khosroyani et al. 2002) to evaluating protocols for vision therapy (Scheiman et al. 2005, Ciuffreda et al. 2008, Carvelho et al. 2008, Shainberg 2010).

By now, five classifications of eye movements have been established: 1) Saccades 2) Vergence 3) Smooth Pursuit 4) Vestibulo-ocular and 5) Optokinetic reflex. Vergence refers to the inward (convergence) and outward (divergence) rotation of the eyes about the vertical axis. The vergence system, which relates to our ability to perceive objects in depth, is investigated in this proposal (and to some extent, saccades as well). Vergence movements are characterized as disconjugate movements in that it involves the rotation of both eyes in opposite directions (Figure 1.1). The purpose of these disconjugate movements is to ensure that an object of interest is projected onto corresponding locations on both retinas (on the foveae) as the eyes are continually rotating inward or outward. The primary focus of this study is to investigate vergence eye movements with respect to multiple measurement modalities: 1) Video-based infrared eye tracking to investigate eye movement dynamics and 2) functional neuroimaging to investigate the neural substrates driving these eye movements.

Humans use vergence eye movements to align their eyes in response to a perceived retinal disparity, or binocular disparity. This disparity, or misalignment, between the projections of the visual scene onto the two retinas is corrected by either

initiating a convergence or divergence movement. While a variety of cues can be used to control the degree of vergence between the eyes (Collewijn, H. & Erkelens, C. J. 1990, Judge S.J. 1991), our primary cue driving these disjunctive vergence eye movements is retinal disparity (Rashbass, C. & Westheimer, G. 1961).

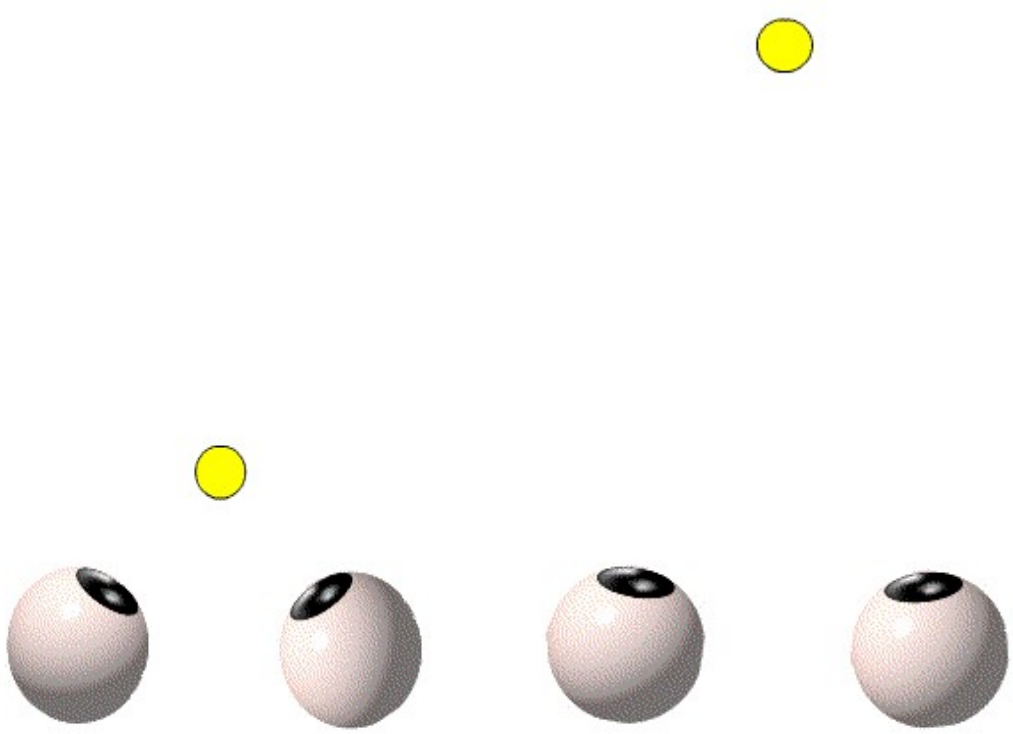

Figure 1.1 Rotation of eyes inward (convergence) and outward (divergence).

Dr. Ernest Edmund Maddox, an ophthalmologist and an early pioneer in the field of impaired binocular vision described vergence as a linear summation of responses to a variety of stimuli (Roper-Hall G. 2009). Dr. Maddox described several components that drive vergence movements: retinal or binocular disparity (vergence error), the state of lens focus (accommodation), proximal cues, and tonic vergence (Maddox EE. 1893).

As the clinical setting focuses on the two primary stimuli to vergence movements, retinal disparity and retinal blur (accommodation), so too does this multimodal investigation in vergence eye movements. To systematize these primary Maddox

components, the effects of disparity stimuli can be isolated and studied while the state of the lens (accommodation) is monitored.

While fusional vergence (retinal disparity-drive) and accommodative vergence (blur-induced) can be studied individually, it should be noted that the two systems indeed interact and work together (Nguyen D et al. 2008). Many studies have revealed the synkinetic relationship between accommodation (A) of the lens and convergence (C) (A. Hughes 1967) where the interaction can be expressed as ratios of the effect of one system on the other (AC/A which describes accommodation-linked convergence and CA/C which describes convergence-linked accommodation).

Although the vergence system can initiate rapid movements with precision to place visual scenes on the retina, there is always some error or disparity. This is referred to as fixation disparity (Fogt N, Jones R 1997), or vergence error. This vergence error, then, serves as a cue or stimulus for disparity-driven vergence (fusional vergence). While Maddox proposed that the accommodative stimulus was the main stimulus to vergence (Maddox EE 1893), current research has shown that fusional vergence is the primary contributor to vergence movements (Horwood AM, Riddell PM 2009, Howard IP, Rogers BJ 2002, Judge SJ 1991, Stark et al. 1980). Due to the arrangement of densely packed cones, the smallest disparities that can be fused is at the fovea centralis.

Neurophysiological studies have been conducted where single cell and lesion studies on primates (Van Horn MR et al. 2013) as well as humans (Sander T. et al. 2009) along with mild and diffuse traumatic brain injury (mTBI and dTBI) in humans (Tyler CW et al. 2015) reveal cortical and subcortical areas involved in vergence eye movements (Figure 1.2).

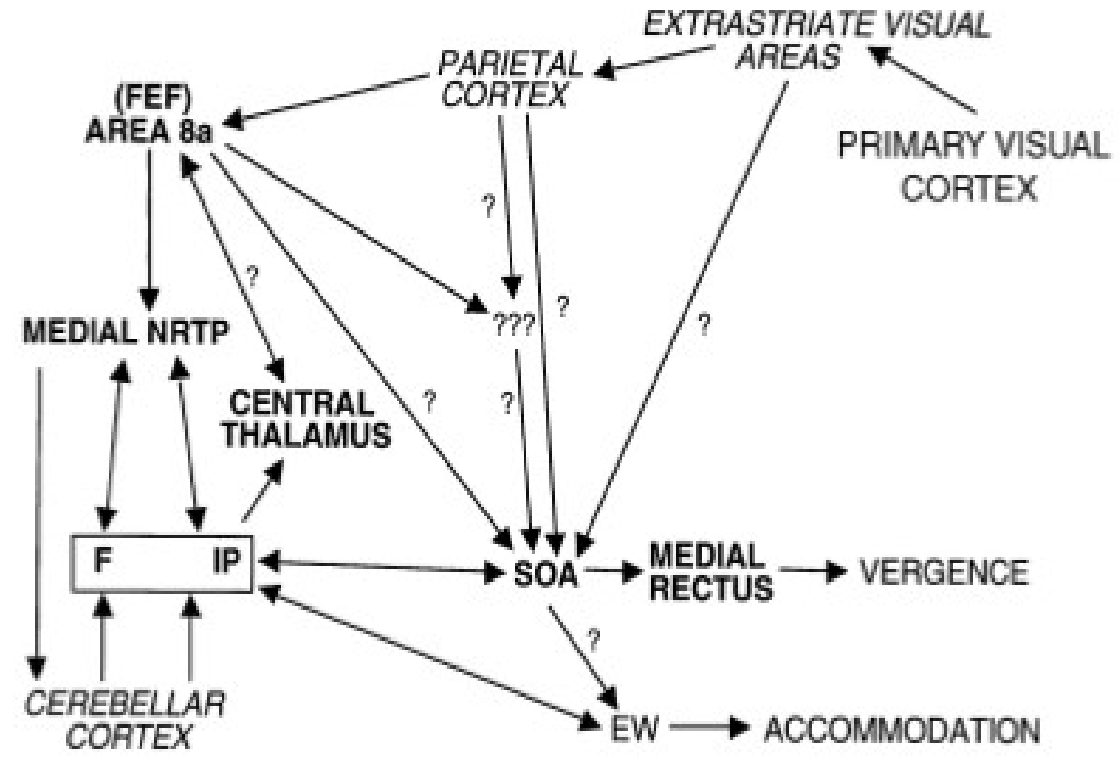

Figure 1.2 Proposed vergence network model that show the neural pathways involved in the control and mediation of vergence eye movements.
Source: Gamlin et al. (2002). Neural mechanisms for the control of vergence eye movements.

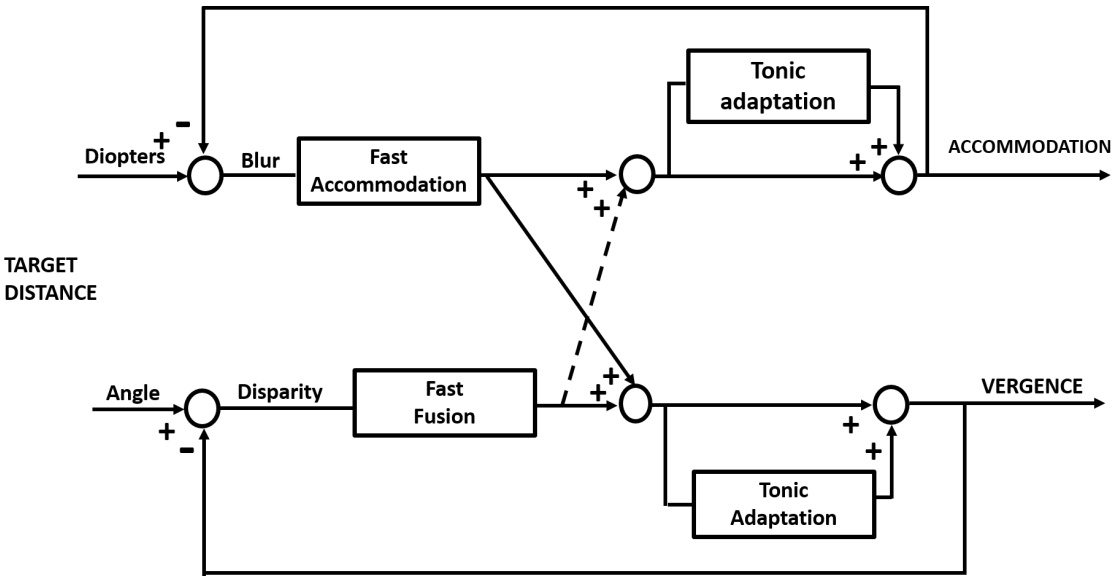

Figure 1.3 System model of the interaction between vergence and accommodation
Source: Schor (1992). A dynamic model of cross-coupling between accommodation and convergence: simulations of step and frequency responses.

1.3 Aims

We propose a multimodal investigation to corroborate the findings of a proposed vergence network model (Gamlin PD and K Yoon 2000, Gamlin PD 2002) by investigating the percent change in the blood oxygenate level-dependent (BOLD) signal in ROIs as well as analyzing the connectivity between these ROIs. In addition, this study aims to provide a foundation for further vergence studies performed in conjunction with fMRI; the repeatability of vergence tasks in fMRI will be assessed. Lastly, this investigation will explore potential asymmetries between left and right eye vergence movements with respect to varying stimuli presentations.

Aim 1A. Study functional activity by analyzing the percent signal change in the fMRI BOLD signal within an ROI.

Aim 1B. Investigate ROI interaction by conducting an ROI-based connectivity analysis between ROIs in binocularly normal controls (BNC) and convergence insufficiency (CI) subjects before and after vergence training.

Aim 2A. Study left eye and right eye vergence peak velocities across varying stimuli presentations.

Aim 2B. Study left eye and right eye vergence latency measures across varying stimuli presentations.

Aim 2C. Investigate phoria as a factor in influencing potential vergence asymmetries.

Aim 2D. Investigate variability in accommodation between left eye and right eye while engaged in vergence eye movements.

Aim 3A. Assess the intraclass correlation coefficient of same-day subject sessions of vergence tasks in fMRI. Assess the interclass correlation coefficient of different-day subject sessions of vergence tasks in fMRI.

Aim 3B. Assess the efficacy of an updated experimental block design for vergence tasks in fMRI with respect to percent signal change in the BOLD within vergence-related ROIs.

Aim 3C. Assess the efficacy of an updated experimental block design for vergence tasks in fMRI with respect to connectivity between vergence-related ROIs.

CHAPTER 2

VERGENCE CONNECTIVITY

2.1 Background and Significance

During routine daily activities, the visual system uses vergence eye movements, which are the inward and outward rotation of the eyes to track objects in three-dimensional space. Several studies support that the posterior parietal cortex (PPC), frontal eye fields (FEF), and cerebellar vermis (CV) are part of the neural network used to mediate a vergence response. (Gnadt JW and LE Mays 1995; Gamlin PD et al. 1996; Sakata H et al. 1999; Ferraina S et al. 2000; Gamlin PD and K Yoon 2000; Taira M et al. 2000; Gamlin PD 2002; Genovesio A and S Ferraina 2004; Alvarez TL, Y Alkan, et al. 2010; Alvarez TL, VR Vicci, et al. 2010; Alkan Y, BB Biswal and TL Alvarez 2011; Alkan Y, BB Biswal, PA Taylor, et al. 2011) However, patients with the binocular dysfunction known as convergence insufficiency (CI) report asthenopia (visual stress) when engaged in near work such as reading. Symptoms for those with CI include: blurred vision, double vision (diplopia), eye strain, reading slowly, and headaches. (Pickwell LD and R Hampshire 1981; Daum KM 1984; Grisham JD 1988; 2008; Scheiman M et al. 2009). FMRI studies have successfully identified which regions of interests (ROIs) are functionally active during a vergence task (Alvarez TL, Y Alkan, et al. 2010; Alkan Y, BB Biswal and TL Alvarez 2011; Alkan Y, BB Biswal, PA Taylor, et al. 2011). Our prior study had reported a decrease in correlation and spatial extent for patients with CI compared to binocularly normal controls (BNC) which increased post vergence training (Alvarez TL, VR Vicci, et al. 2010).

Randomized clinical trials support that repetitive vergence training reduces the visual symptoms of CI patients (Scheiman M et al. 2009; Scheiman M et al. 2011) where the reduction of symptoms is sustained one year post training. (2009) Although clinicians commonly prescribe vergence training (also known as vision therapy or orthoptic exercises) to reduce symptoms, the underlying neuro-physiological basis for improvement in symptoms in CI patients is unknown. (Scheiman M et al. 2011; Cooper J and N Jamal 2012) Our prior published study has shown that after vergence training, CI subjects exhibit an increase in the correlation of the experimental design and the BOLD functional activity as well as a significant increase in functional spatial extent within the FEF, PPC, and CV ROIs compared to pre-training measurements (Alvarez TL, VR Vicci, et al. 2010). Yet, studies have not described how ROIs may exhibit task-modulated co-activation within the vergence neural network in BNC and CI subjects before compared to after vergence training. Several types of connectivity analyses have been developed to study the interaction between ROIs (Biswal B et al. 1995; Margulies DS et al. 2010; Kim SG and S Ogawa 2012).

This study investigated the functional activity and task-modulated co-activation of the neural network used to generate a vergence eye movement. The following hypotheses were tested: 1) significant task-modulated co-activation will be observed between the FEF, PPC and the CV, 2) significantly more functional activity and task-modulated co-activation will be observed in subjects with normal binocular vision compared to those with the CI, and 3) after repetitive vergence training, the functional activity and task-modulated co-activation will improve in CI subjects compared to each subject's baseline measurements. The aims of this investigation are to study functional activity by analyzing the percent signal change in the fMRI BOLD signal within an ROI and to study task-

modulated co-activation by conducting a ROI-based task-modulated co-activation analysis between ROIs in BNC and CI subjects before and after vergence training.

2.2 Research Design

Seven BNC (three females) and four CI (four females) subjects participated in this study. Subjects had no history of brain disorders and were between the ages of 18 and 35 years. Normal binocular vision was defined as having a normal near point of convergence (NPC) less than 8 cm, assessed by measuring the distance a high acuity target was perceived as diplopic along the subject's midline, (Von Noorden GK and EC Campos 2002) and a normal stereopsis (≤ 50 seconds of arc), assessed by the Randot Stereopsis Test (Bernell Corp., South Bend, IN, USA). CI was diagnosed by an optometrist using methods described in our prior study. (Alvarez TL, VR Vicci, et al. 2010) The diagnosis criteria comply with conventional clinical methods. (Cooper JS et al. 2011) All subjects signed written informed consent forms approved by the University of Medicine and Dentistry of New Jersey (UMDNJ) and New Jersey Institute of Technology (NJIT) Institution Review Boards (IRB) in accordance with the Declaration of Helsinki.

The visual stimulus (Figure 2.1) was carefully aligned with the subject's midline to stimulate symmetrical vergence eye movements to test the hypotheses of this study. Subjects could see the targets with the aid of a mirror. Visual stimuli were a set of non-ferrous light emitting diode (LED) targets that formed a line 5 cm in height by 2 mm in width secured with polyvinyl chloride (PVC) tubing. The LED stimulus targets were located at the following three vergence demands: 2°, 3°, and 4°. The target positions were chosen because smaller vergence movements have been shown to elicit fewer

saccadic responses compared to larger vergence movements (Coubard OA and Z Kapoula 2008; Semmlow JL et al. 2008; Semmlow JL et al. 2009; Chen Y-F et al. 2010) as well as due to physical constraints of the scanning room.

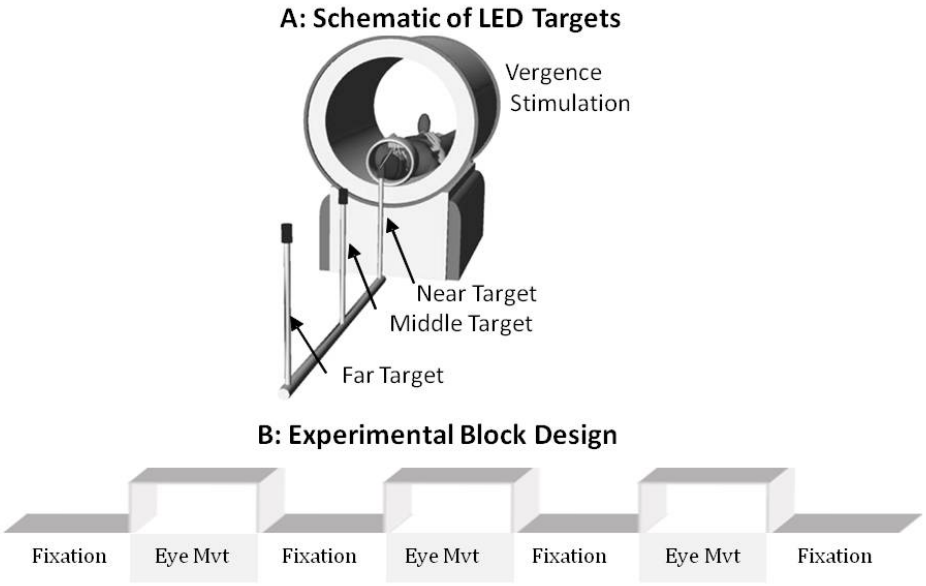

Figure 2.1 (A) Schematic of the LED targets showing visual stimuli. (B) The experimental block design that was composed of sustained fixation (denoted as Fixation) and vergence eye movements (denoted as Eye Mvt) which modulated functional activity of the BOLD signal within the vergence neural substrates.

The experiment utilized a conventional block design of sustained fixation for the 'off' stimulus compared to vergence eye movements for the 'on' stimulus as shown in Figure 2B. Prediction is known to decrease the latency and peak vergence velocity. (Alvarez TL et al. 2002; Kumar AN, Y Han, S Garbutt, et al. 2002; Kumar AN, Y Han, S Ramat, et al. 2002; Alvarez TL et al. 2005; Alvarez TL, Y Alkan, et al. 2010) Hence, to reduce anticipatory or predictive cues, this experiment utilized a series of vergence eye movements where each target was illuminated for a random time between 3 and 5 seconds. LED targets were never simultaneously illuminated. The eye movement

sequence illuminated one of the following three stimuli: the near (4°), middle (3°), or far (2°) target where the subject could not anticipate when the next target would illuminate or which of the three targets would be illuminated. Each phase lasted 20 seconds and was repeated for 3.5 cycles. Hence, the total experiment time was 2 minutes 20 seconds. The experiment was repeated three times per subject.

The AFNI (Cox RW 1996) and FSL (Jenkinson M and S Smith 2001; Jenkinson M et al. 2002) software suites were used to process and analyze the raw data retrieved from the MRI scanner. The first five images of each trial dataset were removed to mitigate the effect of transient scanner artifact. Removal of the first five images to reduce possible T1 stabilization effects is commonly performed within fMRI analyses (Biswal BB et al. 2010).

The AFNI motion correction involves both the removal of spatially coherent signal changes using a partial correlation method, and the application of a six-parameter, rigid-body, least-squares alignment routine. This process yields files from which six motion correction regressors are derived. Three parameters calculate the amount (mm) of movement within each plane (anterior to posterior, right to left, and inferior to superior) and three parameters calculate the amount of rotation (°) between planes (yaw, pitch and roll). These six motion regressors are used within the linear regression model to minimize motion effects of the acquired BOLD signal

The CompCor component data-driven method was used to reduce artifacts found in the BOLD signal. (Behzadi Y et al. 2007) FSL's BET (Brain Extraction Tool) (Smith SM 2002) function removed non-brain tissue from the anatomical image dataset. FSLs FAST (FMRIBs Automated Segmentation Tool) (Zhang Y et al. 2001) stratifies the

skull-stripped anatomical dataset based upon the probability of a voxel being CSF, WM or gray matter (GM). The segmented anatomical CSF and WM probability images were transformed into functional space using FSL's FLIRT function. (Beckmann CF and SM Smith 2004, 2005) To create CSF and WM regressors, CSF and WM probability images all voxels were first assessed using levels of 99% and 97% probability, respectively. The mean time-series were extracted from the voxels surviving the threshold. The probability levels of this study are more conservative compared to those used previously which used a threshold level of 80%. (Biswal BB et al. 2010) Then, the first five principle components relating to CSF and WM were calculated. FSL's FEAT command was used to perform the voxel-wise linear regression analysis on all datasets using the 16 aforementioned regressors (six motion parameters, five principle components of CSF and five principle components of WM). The residuals of the regressed datasets (removal of the 16 artifacts) were then filtered in AFNI using a band pass filter (full width at half maximum (FWHM) Gaussian filter with cut off frequencies of 0.01Hz and 0.15Hz). The band pass filter was used to remove DC offset and high frequency signals that were probably not physiological in nature. All the regressors were removed (leaving the residuals from the regression analysis). Thus, the data sets were motion corrected. This process reduces false positives within this dataset.

A detailed motion analysis of all subjects using a frame displacement method which calculates the absolute value of movement was conducted. (Satterthwaite TD et al. 2013) The frame displacement with one standard deviation for the degree of rotation were 0.18±0.07°, 0.16±0.09°, and 0.20±0.08° for yaw, pitch and roll, respectively. The frame displacement analyzing all subjects within each plane, with one standard deviation, were 0.36±0.13mm, 0.42±0.11mm, and 0.37±.08mm for the anterior to posterior, left to

right, and inferior to superior planes, respectively. Significant differences in motion artifacts were not observed between the post and pre-vergence training data sets of the CI patients assessed using a paired t-test ($p>0.9$). No significant difference in head motion was observed between the two groups ($p>0.9$). Hence, head motion was not considered problematic within this dataset. There were three experimental trials collected in case motion artifact was problematic. A trial that contained considerable motion would be omitted from further analysis. Since our analysis revealed no significant motion artifact, the three experimental trials were averaged per subject after removing the 16 regressors (six motion parameters, five principle components for CSF and five principle components for WM) from each data set.

There were two primary image analyses conducted to test the hypotheses of this study: 1) the average percent signal change per subject within each ROI assessed the functional activity within an ROI and 2) an ROI-based correlation technique of the average ROI time series to assess the task-modulated co-activation between ROIs.

The ROIs were defined using anatomical markers coupled with a model-driven method to identify functional activity near the anatomical markers. Neurophysiology studies on primates supports the following ROIs are involved in vergence eye movements: FEF, PPC and CV. (Gamlin PD et al. 1996; Gamlin PD and K Yoon 2000). This experiment sought to stimulate the cortical and cerebellar regions required to mediate vergence eye movements.

The following ROIs were drawn in native space using anatomical and functional markers: FEF, PPC, and CV. The bilateral FEFs were defined as the area within the intersection between the precentral sulcus and superior frontal sulcus. The PPC was

within the vicinity of the intraparietal sulcus. The CV regions VI and VII were defined on the mid-sagittal plane. Broca's region served as a control ROI because it was not stimulated in prior fMRI vergence studies. (Alvarez TL, Y Alkan, et al. 2010; Alkan Y, BB Biswal and TL Alvarez 2011; Alkan Y, BB Biswal, PA Taylor, et al. 2011) The mask for Broca's region was created using only anatomical markers which are defined near the inferior frontal gyrus anterior to the motor strip. Figure 2.2 depicts the ROIs within a three dimensional brain model used in this study which used axial slices. Table 2.1 lists the volume of each subject's masks for FEF-L, FEF-R, PPC-L, PPC-R, CV, Broca-L, and Broca-R. The average and standard deviation for the masks used are also listed in Table 2.1. The average and one standard deviation of each ROI are shown in Figure 2.2. As Figure 2.2 shows, none of the masks overlap to avoid any partial volume effects. The centroid of the mask listed as left (positive) or right (negative), anterior (positive) or posterior (negative), and superior (positive) or inferior (negative) is denoted within the legend of Figure 2.2.

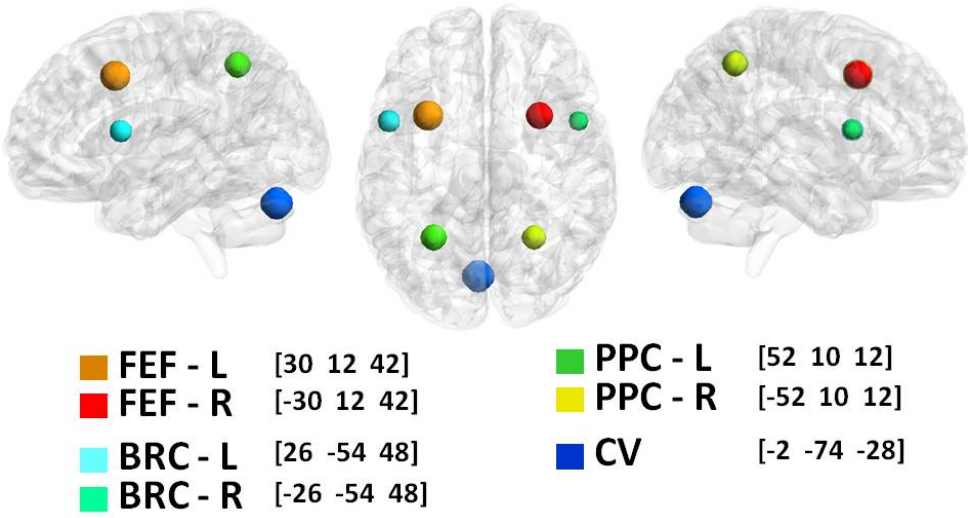

Figure 2.2 Representation of average masks with one standard deviation for the frontal eye fields, left and right [FEF-L (brown) and FEF-R (red)], posterior parietal cortex, left and right [PPC-L (dark green) and PPC-R (yellow)], Broca's region, left and right [BRC-L (light blue) and BRC-R (light green)], and cerebellar vermis [CV (dark blue)] shown using three views within a three-dimensional model brain. The centroid of each mask is denoted as left (positive) or right (negative), anterior (positive) or posterior (negative), and superior (positive) or inferior (negative).

A general linear model (GLM) using a reference time series representation of the block design experimental stimulus convolved with the hemodynamic response function (HRF) was used. Correlation maps were created using a threshold of r □ 0.4 ($p < 0.05$) to show active brain regions. Mask identification was facilitated by observing the active brain regions coupled with the anatomical locations described above for the FEF, PPC and CV. Broca's region was the control ROI and was identified strictly using anatomical markers. Since the datasets were not transformed into a standardized space such as the Montreal Neurological Institute (MNI) space, some variance is also observed for the mask of Broca's region.

Broca's region served as a control ROI (not related to the hypotheses of this study). Language was not manipulated within the experimental protocol. Prior

investigations show Broca's region was stimulated during experiments that study language (Geschwind N 1970; Kim KH et al. 1997) but is not stimulated within vergence eye movements experiments. (Alkan Y, BB Biswal and TL Alvarez 2011; Alkan Y, BB Biswal, PA Taylor, et al. 2011) To further enhance the study, Broca's region was used as a control ROI to study the variability within a non-stimulated ROI. The Broca mask only used anatomical markers to pool the time series from that region since the BOLD signal did not significantly correlate to the experimental design.

All data were kept in native space (i.e., data were not transformed into Talairach & Tournoux or Montreal Neurological Institute (MNI) space) to reduce any warping artifacts. The time series located within the vicinity of the anatomical markers, which had a Pearson correlation coefficient of $r \leq 0.4$ ($p < 0.05$) with the hemodynamic model described above, were pooled. This study used a within subject longitudinal design. The same threshold was used on the pre and post vergence training analysis. Therefore, we assume that any potential differences observed within the data sets were due to training. The BOLD percent signal change for each ROI per subject comparing elevated activation observed during the vergence task to the baseline of sustained fixation was computed from the time series. The individual-subject percent signal change values were pooled to conduct the group-level statistical analysis described below. The time series from each ROI were also correlated with the square wave experimental block design to compute Pearson Correlation values.

Using the averaged signal from each ROI described above, a task-modulated co-activation analysis was conducted. A pair-wise correlation was computed using the averaged time series for each ROI per individual subject. The MATLAB software suite

(Waltham, MA, USA) was used to perform a pair-wise linear correlation analysis between the following seven ROIs: left and right frontal eye field (FEF-L, FEF- R), left and right posterior parietal cortex (PPC-L, PPC-R), cerebellar vermis VI and VII (CV), and left and right Broca's region (BROCA-L, BROCA-R). This analysis was conducted on the seven BNC and the four CI subjects before and after vergence training. These data were then pooled to conduct a group-level analysis. A correlation matrix was plotted using the mean values from each of the three groups studied (BNC, CI before and CI after vergence training).

Repetitive vergence training was utilized to provoke changes in the neural substrates that stimulate vergence eye movement responses. The CI subjects participated in a total of 18 hours of vergence training, 6 hours at home and 12 hours in the laboratory. Home training was monitored by having each CI subject record in a log book the amount of time spent on training. It entailed two 10-minute sessions (morning and evening) three days per week for six weeks. Laboratory training was composed of one-hour sessions, twice per week for six weeks. Within a single day, a subject participated in either laboratory or home training but not both. Details of the vergence training were described in our previous publication (Alvarez TL, VR Vicci, et al. 2010). The laboratory and home training consisted of step and ramp stimuli similar to methods used clinically (Griffin JR 1988; Scheiman M and B Wick 2008).

Symptoms were quantified using the Convergence Insufficiency Symptom Survey (CISS), which is a 15 question survey.(2008) Each symptom is scored between zero to four where zero represents the symptom never occurs and four represents the symptom occurs very often. The responses are summed where a score of 21 or higher has been

validated to have a sensitivity of 98% and specificity of 87% in young adults between 18 and 35 years of age. (Rouse MW et al. 2004)

The subject data were stratified into the following three groups: BNC, CI subjects before vergence training, and CI subjects after vergence training. An unpaired t-test was used to determine whether significant differences were observed in 1) the percent signal change of the BOLD fMRI signal within an ROI and 2) the task-modulated co-activation between ROIs by comparing the CI and the BNC groups. A paired t-test determined whether the CI subjects exhibited significant changes in the percent signal change of the fMRI BOLD signal within an ROI, task-modulated co-activation between ROIs, CISS, near point of convergence, vergence ranges, and near dissociated phoria, for the post vergence training measurements compared to pre-training measurements. Linear regression was conducted between 1) the CISS and the BOLD percent signal change and 2) the CISS and the task-modulated co-activation where the Pearson correlation coefficient was assessed for significant correlation. Statistics were calculated using NCSS2004 (Kaysville, UT, USA). Significance was defined as a p-value < 0.05. Bonferroni correction was not applied because of the limited number of subjects within the study. Figures were generated using MATLAB (Mathworks, MA).

2.3 Results

A paired t-test revealed a significant difference comparing the baseline (before vergence training) parameters and the after vergence training parameters for the following measurements: the near point of convergence (NPC) ($t = 4.9$; $p = 0.04$), base out (BO) positive fusional vergence range ($t = 9.5$; $p = 0.01$), near dissociated phoria ($t = 11$; $p = 0.008$), and CISS ($t = 3.6$; $p = 0.05$). All significant changes are improvements to the clinical signs and symptoms studied.

Figure 2.3 shows data from two subjects whose individual parameters were most similar to the group averages, one BNC (left column), one CI subject before vergence training (middle column), and the same CI subject after vergence training (right column). Figure 4A shows the average time series from the FEF-L (red line) and the PPC-L (green line) plotting the percent signal change as a function of volumes collected (a total of 70 volumes equating to 140 seconds in duration). The thickness or absence of a yellow line between ROIs in Figure 2.3B represents the strength and significance of the task-modulated co-activation. Each line is labeled with the Pearson correlation coefficient and p value derived from the correlation between the following ROIs: FEF-L, PPC-L, Broca-L and the CV denoted as the red, green, purple and blue circles, respectively. Note, Broca-L has no lines to the FEF-L, PPC-L and CV because the task-modulated co-activation was not significant ($p>0.01$) in these two subjects shown or in any of the other subjects analyzed. Figure 2.3C shows the time series from Broca-L (purple lines) and from the CV (blue lines). The BNC shows an FEF time series which is more correlated ($r = 0.66$; $p<0.001$) with the experimental block design (white and gray boxes for the 3.5 cycles of the experiment) compared to the CI before vergence training ($r = 0.33$; $p<0.01$).

After vergence training, this subject's FEF correlation with the block design increases ($r = 0.73$; $p<0.001$). Similar trends are observed for the PPC and the CV. As expected, the time series from Broca's region (control ROI to study variability of a non-stimulated region) does not correlate with the experimental block design for the BNC and the CI before or after vergence training ($r = 0.15\pm0.05$; $p>0.1$).

Figure 2.3B shows the ROI-based task-modulated co-activation analysis for two individual subjects, one BNC and one CI before and the same CI after training. The average time series were significantly correlated between the FEF and PPC, FEF and CV, and PPC and CV for the BNC ($r>0.71$; $p<0.001$). However, for the BNC, the time series from Broca's region was not significantly correlated to FEF, PPC or CV, displayed without a line between Broca's region (purple circle) and the other ROIs ($r<0.1$;$p>0.2$). Figure 4B shows the data from CI subject 3, who had the highest task-modulated co-activation within the CI group before vergence training. Even for this CI subject (before training), the task-modulated co-activation ($0.18 < r < 0.44$) was less compared to the BNC subjects. For this same CI subject after vergence training, the correlations between the FEF, PPC and CV improved ($r>0.63$; $p<0.001$) compared to the baseline measurements. For the CI subject before and after vergence training, the time series from Broca's region did not correlate to any of the other ROIs ($r<0.2$; $p>0.05$). The width of the yellow line represents the level of significance. High significance ($p<0.001$) is denoted using a thick line and lower significance ($0.001< p <0.05$) is denoted using a thin line.

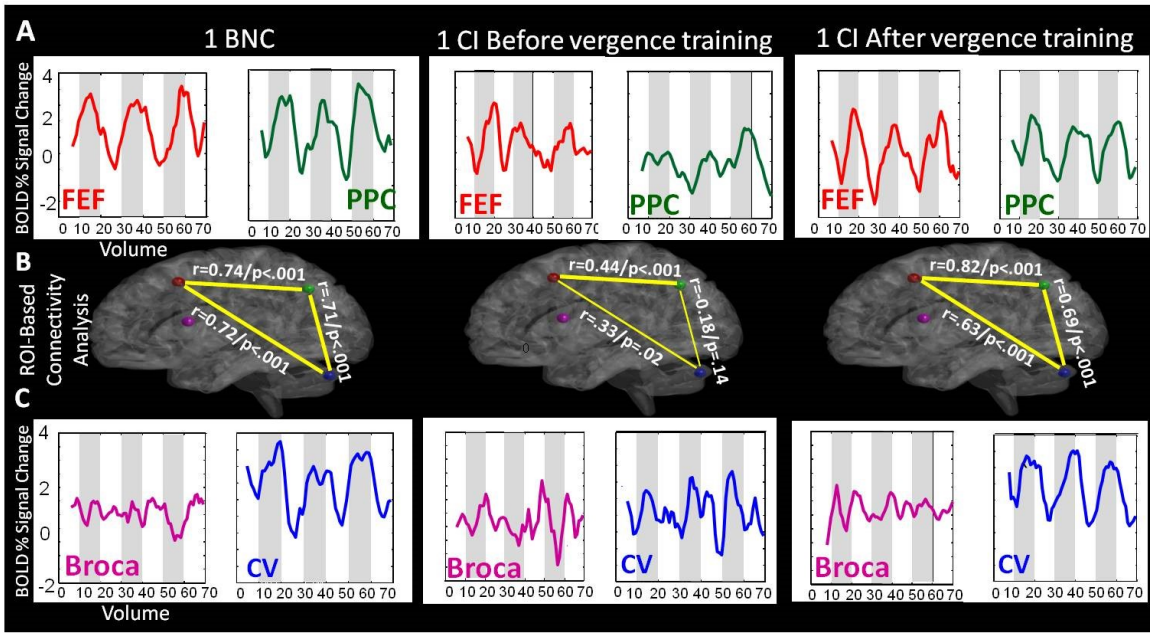

Figure 2.3 (A) Averaged time series for the FEF-L (red) and PPC-L (green) ROIs from one typical BNC (left) and one CI before (middle) and the same CI after vergence training (right). (B) Example of the task-modulated co-activation analysis between FEF-L (red circle) PPC-L (green circle), CV (blue circle) and Broca-L (purple circle). The Pearson Correlation coefficient (r value) and p value are shown where the thickness of the line represents the significance. The time series from Broca-L was not significantly correlated to FEF-L, PPC-L or CV in any of the subjects studied. (C) Averaged time series for Broca-L (purple) and CV (blue).

Figure 2.4 shows the average with one standard deviation for the group-level analysis of the percent change in the BOLD signal per ROI for the following groups: BNCs (green bar), CI subjects before vergence training (blue bar) and CI subjects after vergence training (red bar). When comparing the BNC to the CI data before vergence training using an unpaired t-test, significant differences were observed within the FEF, PPC and CV ($t > 2.3$; $p < 0.05$). Significant differences were not observed within Broca's region between the BNC and either the before or after vergence training CI datasets ($t > 1.1$; $p > 0.3$). A paired t-test showed the percent change in the BOLD signal in the FEF, PPC and CV of the four CI subjects who participated in vergence training were significantly greater after training compared to the baseline values ($t > 2.6$; $p <$

0.001). No statistical difference was observed in Broca's region ($t = 1.2$; $p > 0.3$) when comparing the baseline and after vergence training data.

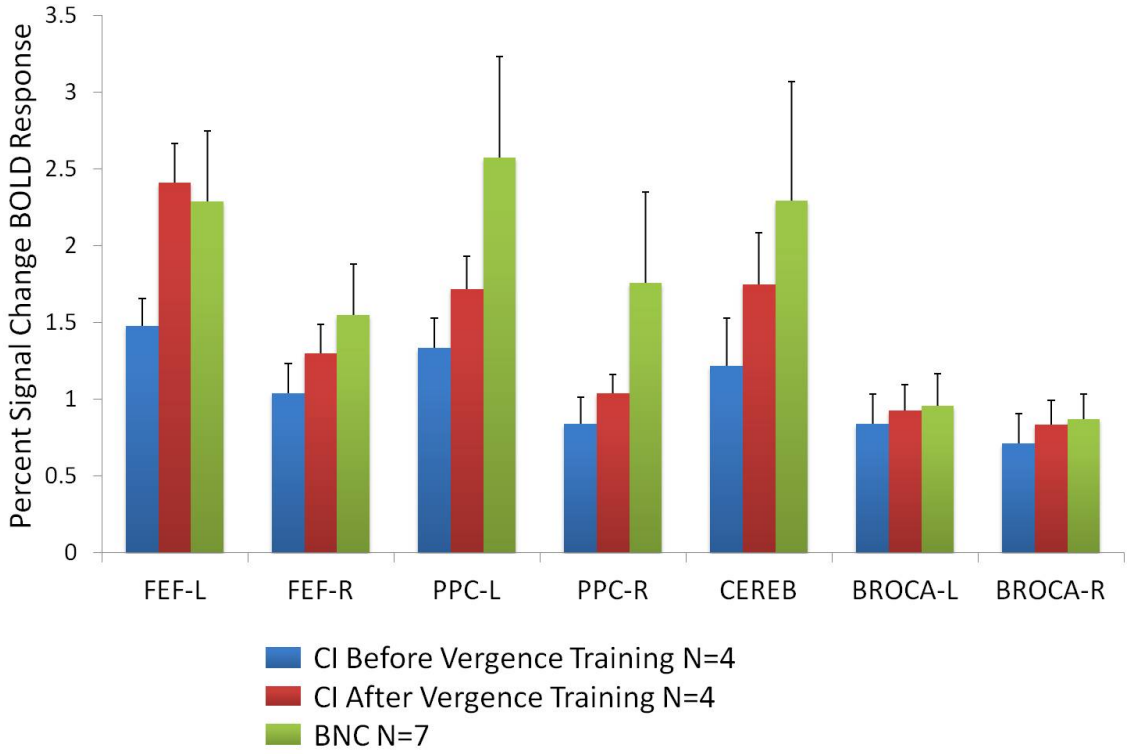

Figure 2.4 Percent BOLD signal change for FEF-L (Left), FEF-R (Right), PPC-L, PPC-R, CV, Broca-L, and Broca-R for CI subjects before vergence training (blue), CI subjects after vergence training (red) and the BNC subjects (green). Bar plots are the average plus one standard deviation.

Figure 2.5A shows a correlation matrix of the group-level BNC dataset. The color bar represents the average correlation between the ROIs labeled in the row versus the column. In the BNC group, strong correlations were observed between the left and right FEF, left and right PPC, and the CV. The time series from Broca's region was not significantly correlated to the FEF, PPC or CV ($r < 0.2$; $p > 0.1$). Figure 2.5B and 2.5C shows a correlation matrix for the group-level CI dataset before and after vergence training, respectively. For the CI subjects, correlation values between the FEF, PPC and

CV were lower before vergence training and these values increased post vergence training. Figure 2.5 plots D through F displays the p-values for the following statistical comparisons that were conducted: unpaired t-test comparing BNC versus the CI before vergence training datasets, an unpaired t-test comparing the BNC and the CI after vergence training datasets, and a paired t-test comparing the CI before and after training datasets. The task-modulated co-activation of the BNC group was significantly different compared to the task-modulated co-activation of the CI group before vergence training dataset for the FEF, PPC, and CV. After vergence training, the CI group dataset was not significantly different compared to the task-modulated co-activation of BNC group dataset. The paired t-test comparing the before and after vergence training CI datasets revealed that a significant increase of task-modulated co-activation was observed between the CV and the PPC-L ($p<0.05$).

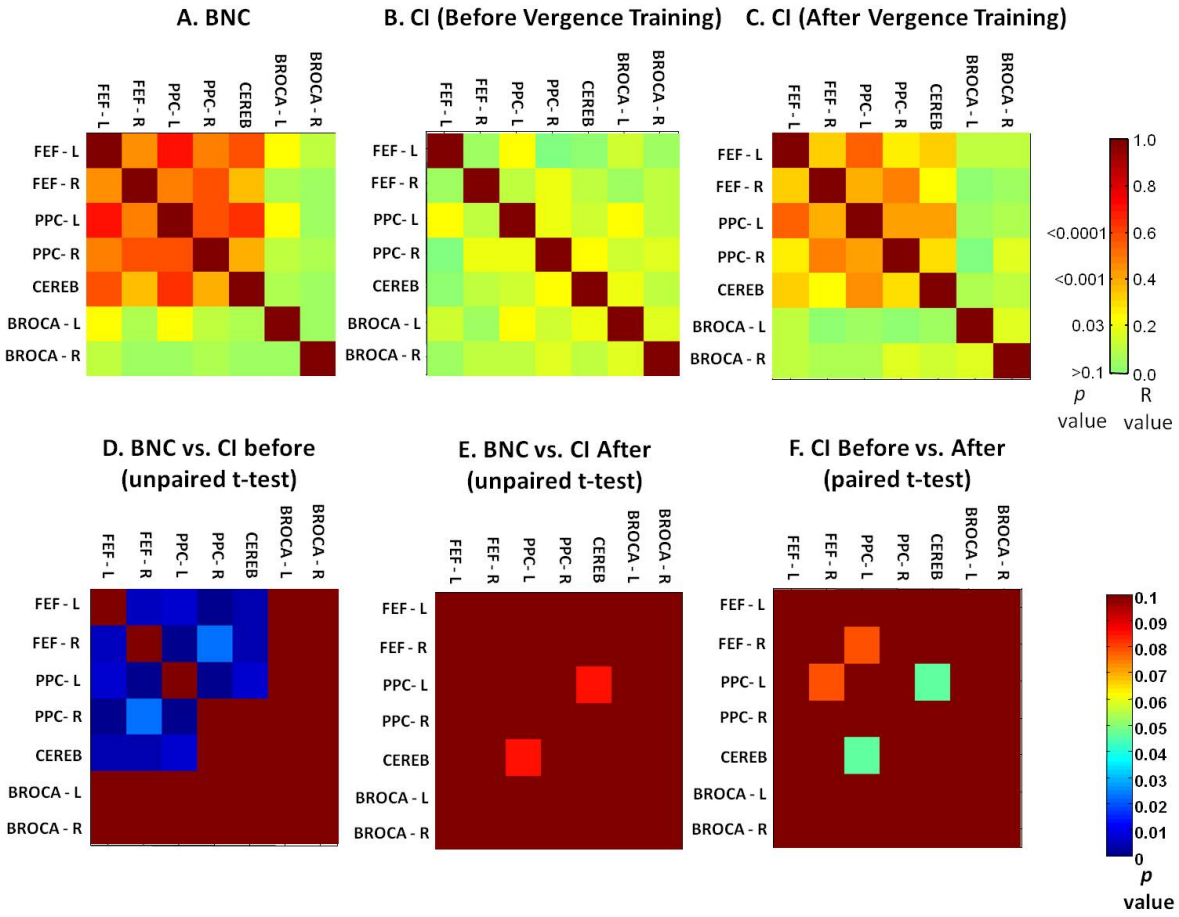

Figure 2.5 Pair-wise correlation analyses. Group-level correlation values are between FEF (left and right), PPC (left and right), CV and Broca's Region (left and right) for BNCs (A), CI subjects before vergence training (B) and the same CI subjects after vergence training (C). Group-level statistical comparisons reporting p-values are shown for BNC versus CI-Before (D), BNC versus CI-After (E), and CI Before versus CI-After

The linear regression analyses reported that for the CI datasets, the CISS and the percent BOLD signal change from the following ROIs: FEF-L (Figure 2.6A), FEF-R (Figure 2.6B) and CV (Figure 2.6C), were significantly correlated ($r \leq -0.7$; $p < 0.02$). The correlations between CISS and the following ROIs: PPC-L, PPC-R, Broca-L and Broca-R were not significant ($-0.6 \leq r \leq 0.4$; $p > 0.1$). Linear regression analyses were also conducted on the differences between the percent change in the BOLD signal as a function of the differences in the CISS. Difference was defined as the measurements

after vergence training minus the initial measurements before vergence training. The sample size is small where none of the correlations were significant ($p>0.1$). However, the correlation for the difference in the BOLD percent signal change for the cerebellum ROI as a function of the difference in CISS had a Pearson correlation coefficient of $r=0.8$. Linear regression analyses were also conducted to assess the correlation between the task-modulated co-activation and the CISS. Significant correlations between the task-modulated co-activation of each pair of ROIs and the CISS were not observed ($-0.6 \leq r \leq 0.4$; $p > 0.05$). The greatest correlation was observed between the CISS and the task-modulated co-activation between the right FEF and left PPC ($r = -0.65$; $p=0.08$).

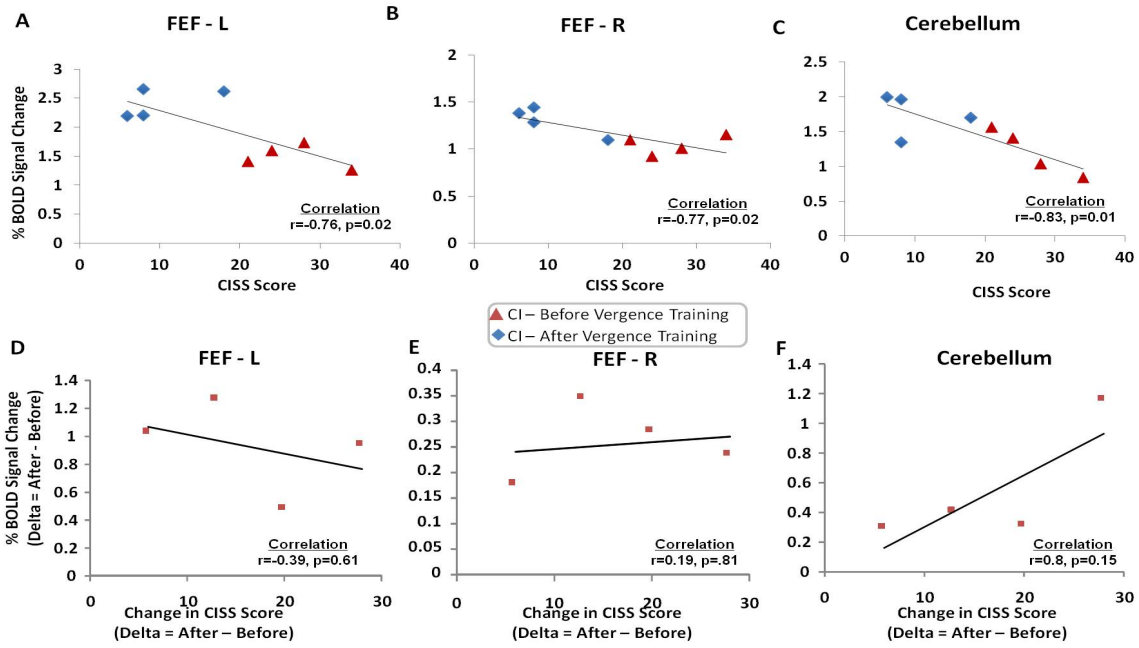

Figure 2.6 Statistically significant linear regression analyses. Percent BOLD signal change versus CISS scores for CI groups (before and after vergence training) for the FEF-L (A), FEF-R (B), and CV (C). Linear regression analyses for the difference in the percent BOLD signal change (measurements after vergence training minus measurements before vergence training) as a function of the change in the CISS score (after minus before vergence training) for the FEF-L (D), FEF-R (E), and cerebellum (F).

2.4 Discussion

The data support the hypotheses that were tested. Significant task-modulated co-activation was observed between the FEF, PPC and CV ($p<0.05$) in BNC subjects. Functional activity and task-modulated co-activation studying the FEF, PPC and CV assessed via the percent BOLD signal change and an ROI-based correlation analysis, respectively was reduced in CI subjects before vergence training compared to BNCs. After vergence training, both functional activity and task-modulated co-activation between the FEF, PPC and CV significantly increased in CI subjects. Broca's region was not significantly different between the BNC and the CI subjects (using either the before or after training data). The results of this study will be compared to those in the literature.

Non-human primate single cell electrophysiology studies have investigated the influence of disparity in FEF using symmetrical step stimuli (Gamlin PD and K Yoon 2000), near and far targets (Ferraina S et al. 2000), and smooth sinusoidal tracking stimuli (Fukushima K et al. 2002; Akao T et al. 2005). The FEF and PPC have also been shown to be involved in predictive oculomotor learning. (Tseng P et al. 2013) The PPC encodes for different binocular distances defined by different vergence angles studying primates using single cell recordings (Genovesio A and S Ferraina 2004; Ferraina S et al. 2009; Breveglieri R et al. 2012) and humans using transcranial magnetic stimulation (Kapoula Z et al. 2001; Kapoula Z et al. 2004; Yang Q and Z Kapoula 2004; Kapoula Z et al. 2005) and fMRI. (Quinlan DJ and JC Culham 2007; Alvarez TL, Y Alkan, et al. 2010; Alkan Y, BB Biswal and TL Alvarez 2011; Alkan Y, BB Biswal, PA Taylor, et al. 2011) Primate single cell studies have also shown that the cerebellar vermis is used to mediate a vergence response. (Gamlin PD et al. 1996; Nitta T et al. 2008, 2008)) Patients,

particularly those with lesions to the cerebellar vermal regions, exhibit a decrease in slow tracking vergence.(Sander T et al. 2009)

This present study further confirms that the FEF, PPC and CV are metabolically active during a vergence task. The novelty of this study's results is that the functional activity of the FEF, PPC and CV are reduced in CI subjects at baseline compared to BNC subjects and significantly improved after 18 hours of vergence training to levels more similar to those exhibited by the BNC subjects. The results support the hypothesis that subjects with CI have reduced functional activity compared to BNC and that after vergence training the functional activity improves to levels more similar to those observed in BNC.

The task-modulated co-activation of the vergence network is not completely understood. Neurophysiology studies on primates support a direct connection between the FEF and PPC as well as a connection between the FEF and cerebellar cortex through the nucleus reticularis tegmenti pontis (NRTP). (Gamlin PD 2002) Functional connectivity studies using resting state fMRI support connectivity between the FEF and PPC studying humans and primates. (Hutchison RM et al. 2012) In addition, direct connections between the lateral intraparietal area (LIP) and the oculomotor cerebellum have been identified using a combination of rabies virus and a conventional cholera toxin B tracer in nonhuman primates. (Prevosto V et al. 2010). The present study implies the FEF, PPC and cerebellar vermis may have functional connections quantified through the task-modulated co-activation analysis.

Information is scarce in terms of how task-modulated co-activation may be altered for those with CI. This present study supports the hypothesis that task-modulated

co-activation on average is significantly lower compared to task-modulated co-activation observed within BNC subjects. However, after 18 hours of vergence training, CI patients exhibited significant correlation between the FEF, PPC and CV ROIs showing task-modulated co-activation patterns more similar to BNC subjects thus supporting the third hypothesis. These data suggest that vergence training not only increases the percent BOLD signal change within the FEF, PPC and CV but also increases the task-modulated co-activation between the PPC and CV ROIs. Increasing the correlation of the BOLD signal within and between the FEF, PPC and CV may be one mechanism that leads to the sustained reduction in visual symptoms CI subjects experience after vergence training. These data support that the CISS was significantly correlated to the BOLD percent signal change within the FEF and CV. These data suggest that future therapeutic interventions may consider targeting the improvement of the metabolic activity within FEF and CV.

The techniques developed within this study can serve to compare different vergence training protocols to provide a deeper understanding of the mechanisms evoked during vergence training and serve to compare future vergence training protocols. Ultimately, the techniques within this study have the potential to evaluate the efficacy of different therapeutic protocols leading to further improvements in vision function.

While eye movement rehabilitation studies utilizing fMRI are scarce, fMRI has been used to study the effects of rehabilitative training tasks that use eye movements such as reading. (Shaywitz SE et al. 2003; Laatsch LK et al. 2004; Laatsch L and C Krisky 2006) One study investigated a saccadic task and reading comprehension task before and after cognitive rehabilitation therapy where functional activity increased post therapy compared to the baseline measurements studying patients with mild (Laatsch LK et al.

2004) and severe (Laatsch L and C Krisky 2006) traumatic brain injury. Reading investigations in dyslexic patients showed reduced activation in the left parietotemporal and occipitotemporal regions in patients who did not improve their reading ability compared to dyslexic patients who did improve their reading in adulthood. (Shaywitz SE et al. 2003) Another study on vision restoration training has shown an increase in visual receptive fields correlated to an increase in the amplitude of the BOLD signal in patients with cerebral blindness.(Raemaekers M et al. 2011) Similar to the prior reading, saccade and vision restoration training protocols, this current study also reports an increase in functional activity assessed via the BOLD percent signal change compared to each subject's baseline measurements.

Functional connectivity has become more common within longitudinal studies to investigate whether the interaction between ROIs is an independent factor which may contribute to the sustained improvement observed in rehabilitation. The present study was novel because it was the first to analyze task-modulated co-activation for those with CI undergoing repetitive vergence training. For brain injury patients, studies have shown a decrease in functional connectivity three months post injury compared to neurologically normal subjects where functional connectivity improved to levels more similar to controls six months post injury. (Nakamura T et al. 2009) For patients with multiple sclerosis, the increase in functional connectivity assessed as an increase in correlation between ROIs, predicted the effects of cognitive rehabilitation quantified via assessment of attention, executive function, depression and quality of life (Parisi L et al. 2013) as did another study that used the modified Story Memory Technique. (Leavitt VM et al. 2012) Patients with stroke also exhibited a decrease in functional activity post stroke (within the first month) and connectivity was improved post rehabilitation where functional

connectivity was significantly correlated to motor function. (Park CH et al. 2011; Golestani AM et al. 2013) For healthy individuals, learning a novel motor task resulted in an increase in functional connectivity within the fronto–parietal network after repetitive training of the motor task. (Taubert M et al. 2011) In summary, prior rehabilitative interventions in those with brain injury, stroke and multiple sclerosis all report that an increase in functional connectivity is correlated to an improvement in behavioral function. Similar to the aforementioned functional connectivity studies, this current study supports that an increase in task-modulated co-activation after 18 hours of vergence training was observed compared to baseline measurements in CI subjects.

When studying sensory, motor and cognitive function, several fMRI investigations conclude that fMRI has high test-retest precision (Gamlin PD et al. 1996; Yetkin FZ et al. 1996; Brannen JH et al. 2001; Loubinoux I et al. 2001; Kiehl KA and PF Liddle 2003; Specht K et al. 2003; Peelen MV and PE Downing 2005; Yoo SS et al. 2005; Zou KH et al. 2005; Freyer T et al. 2009). Similar results are reported for resting state fMRI studies (Shehzad Z et al. 2009; Meindl T et al. 2010; Blautzik J et al. 2012; Song J et al. 2012). A recent eye movement study of the reliability of a saccadic task showed an interclass correlation coefficient of greater than 0.5 in 75% of the subjects studied. (Ming J et al. 2012) Furthermore, studies report that reliability is improved when movement artifacts are small (Lund TE et al. 2005) and that 3T scanners have better repeatability compared to 1.5T scanners (Zou KH et al. 2005).

This study has a small sample size and future studies should evaluate whether the results observed here generalize to a larger population. It is unknown whether the changes observed immediately after therapy persist long term. We would anticipate the

observed functional changes would be sustained because a randomized clinical trial studying CI patients reports that the reduction in CISS continues one year post vergence training. (2009) Ideally, future studies will include a larger scale randomized clinical trial composed of four groups. Half of the subjects would be BNC and the other half would have CI. Half the BNC and half of the CI subjects would participate in active vergence training while the remaining BNC and CI subjects would receive placebo training. This type of study is beyond the resources of this present study.

While the present study used Broca's Region as a control ROI to study the variability within fMRI, future studies should also assess the repeatability of functional activity stimulated with vergence eye movements within BNC subjects. A repeatability investigation of functional activity evoked from saccadic eye movements using 45 subjects reports activation consistency between 60-85% within the same subject. (Lukasova K et al. 2013) Hence, we suspect the test-retest analysis of vergence will be similar to that observed within saccadic studies.

2.5 Conclusion

The data of the present study support that CI subjects had a decrease within the percent BOLD signal change within the FEF, PPC and CV compared to BNC subjects which improved to levels more similar to BNC subjects after 18 hours of vergence training. The task-modulated co-activation between the FEF, PPC and CV was also reduced in CI patients compared to BNC and improved post vergence training. The CISS was significantly correlated to the BOLD percent signal change within the FEF and CV. Results support that an increase in functional activity within and task-modulated co-activation between the FEF, PPC and CV ROIs may in part lead to the sustained reduction in symptoms assessed via the CISS reported by CI subjects.

CHAPTER 3

VERGENCE ASYMMETRY

3.1 Background and Significance

Over a century ago, Rosenbach (1903), brought forth the idea of people having a dominant eye. To test his idea, a simple vision task was performed where a person would be instructed to aim their index finger at a distant object while both eyes were opened. Since that index finger would be imaged outside of panum's fusional area, it would appear doubled and so the subject would be forced to choose one finger over the other. What Rosenbach found was that, indeed, most people preferred the image of one eye to the other.

Interestingly enough, Wall (1951) showed that the preferred eye in Rosenbach's vision task was not necessarily the eye with higher visual acuity. Hillesman (1927) corroborated Rosenbach's results in a study of 400 subjects, where 40% preferred their right eye, 20% preferred their left eye, and 40% were unsure which image they preferred.

Prior studies have investigated asymmetries in vergence eye movements. Semmlow, et al. (1998) studied asymmetries in pure symmetric vergence eye movements and found that although both eyes eventually arrive at symmetrically convergent positions, the initial portions of the movements showed differences in amplitude and peak velocity. Alvarez et al. (2012, 2013) showed that the frequency of saccades are correlated to vergence peak velocity in binocularly normal controls as well as those with convergence insufficiency.

This study seeks to investigate factors that influence ocular dominance. Specifically, we investigate the potential effects of varying stimulus size and color on vergence eye movements.

3.2 Research Design

Fifteen subjects (9 male, 6 female) participated in this study. All subjects had no history of binocular dysfunction and were between the ages of 18 and 35 years. Normal binocular vision was defined as having a normal near point of convergence (NPC) less than 6cm, which was assessed by measuring the distance a high acuity target, was perceived as diplopic along the subject's midline (Von Noordern GK and EC Campos 2002) and a normal stereopsis (≤ 50 seconds of arc), assessed by the Randot Stereopsis Test (Bernell Corp., South Bend, IN, USA). All subjects signed written informed consent forms approved by the New Jersey Institute of Technology (NJIT) Institution Review Board (IRB).

Figure 3.1A illustrates stimuli size and color utilized in this study. With three different stimuli sizes and four possible color pairings presented to the left and right eye, twelve observations are made per trial. The size of the stimuli pair is chosen after carefully reviewing retinal eccentricity plots (Figure 1b). Three stimuli pairs are used where they range in width from 2°, 4°, and 6° in length and height. In order to investigate the effect of stimulus size, our experimental stimuli are created with control of degree of foveal stimulation in mind.

In addition to stimulus size, the shape of the stimulus itself is considered. The "cross" stimuli pairs used in observations 1-4 (Figure 3.1b) are not only small in size (2° length x height), but are also meant to demand focus centrally. While observations 5-8

(4°) and 9-12 (6°) are designed to be larger in size, their "eccentric circle" shape are clinically derived and are meant to be a more rich and salient visual stimulus that engages the regions of the retina that extend just beyond the acute fovea centralis.

Apart from size, the color of the stimuli is also investigated across all twelve observations. As determined by the retinal eccentricity plot (Figure 3.1B), stimulus size is meant to induce stimulation starting at the fovea centralis, moving further peripherally as the stimuli targets become larger. The fovea centralis, or central region of the retina, is populated exclusively by cones (Cicerno et al. 1989, Gowdy et al. 1998, Krauskopf et al. 2000), which allow for color vision and are responsible for rendering high spatial acuity. Currently there is a great deal of research involving the determination of the ratios of cone types and their arrangement throughout the retina (Chui et al. 2012, Lombardo et al. 2013, Park et al. 2013, Song et al. 2011). Although prior studies involving vision tracking have used blue stimuli, this study investigates vergence eye movements with respect to red and green stimuli. As seen in cone mosaics of the retina (Figure 3.2), the fovea is predominantly populated by medium-wavelength (green) and long-wavelength (red) cones. Prior studies have investigated the human trichromatic cone mosaic in order to better understand the properties of the network of cones that allow us to derive color across a spectrum of light [Hofer et al. 2005]. Among the three cone types found in our retina (short-wavelength (S), medium-wavelength (M), long-wavelength (L)), the M and L cones are in greater abundance than the S. As a result, our stimulus colors were chosen to reflect this physical fact.

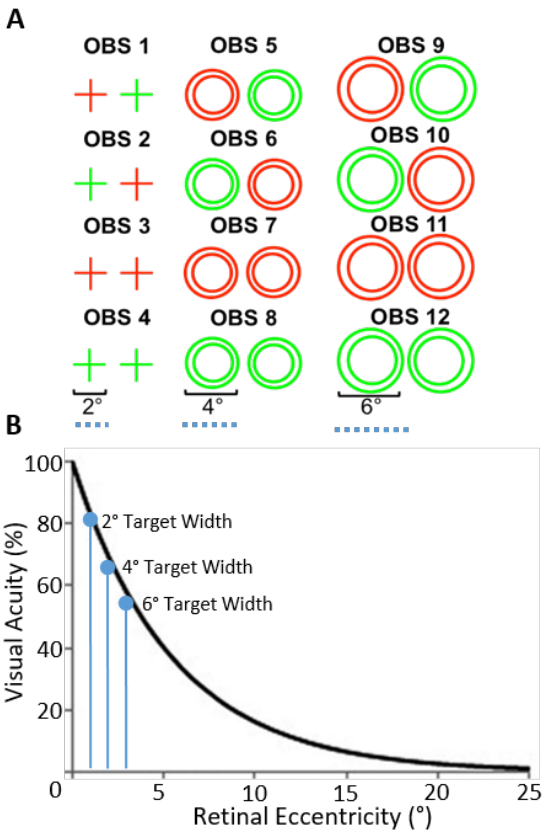

Figure 3.1 A) Stimulus design used in this study with respect to size and color. As pictured, there are twelve unique observations in total. B) A retinal eccentricity plot. The further away from the fovea, the density of cones and hence, visual acuity, decreases exponentially.

While Figure 3.1B highlights retinal eccentricity, influencing our stimulus design in terms of size, figure 2.9 shows the approximate contribution to overall cone absorption from the three groups, or chromatic aberration. It has been shown that the fovea is composed of entirely cones. Specifically, the makeup of the fovea finds there to be almost exclusively M (green) cones and L (red) cones (Figure 2.10). Although prior studies involving vision tracking have used blue stimuli, this study will investigate asymmetrical differences between the fovea, parafovea, and perifovea with respect to red and green stimuli.

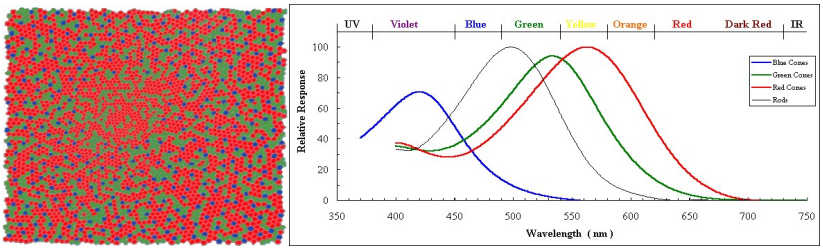

Figure 3.2 A) A cone mosaic of the fovea centralis highlights the densely packed population of cones in the region. Note the prevalence of M (green) and L (red) cones. B) This graph shows the approximate contribution to overall cone absorption from the three groups. Each cone type detects a different range of wavelength. Between them, they discern all wavelengths from about 380 nm to 760 nm, producing the greatest sensitivity at around 555 nm.

Source: Sharpe, L. T., Stockman, A., Jägle, H., & Nathans, J. (1999). Opsin genes, cone photopigments, color vision and colorblindness. In K. Gegenfurtner & L. T. Sharpe (Eds.), Color vision: From Genes to Perception (pp. 3-51) Cambridge: Cambridge University Press.

Eye movements are recorded using a custom-built haploscope (Figure 3.3). The haploscope employs two-way mirrors that project left eye and right eye stimuli into opposing visual fields. This forces the subject to make a vergence movement to attain target fusion. The ISCAN (Figure 3.3A) infrared tracking instrument records the induced vergence eye movement of each eye with a sampling rate of 500Hz. The haploscope allows for isolation of the fusional vergence component, where stimulation of the accommodative system is held relatively constant (Kotulak J.C. et al. 1986).

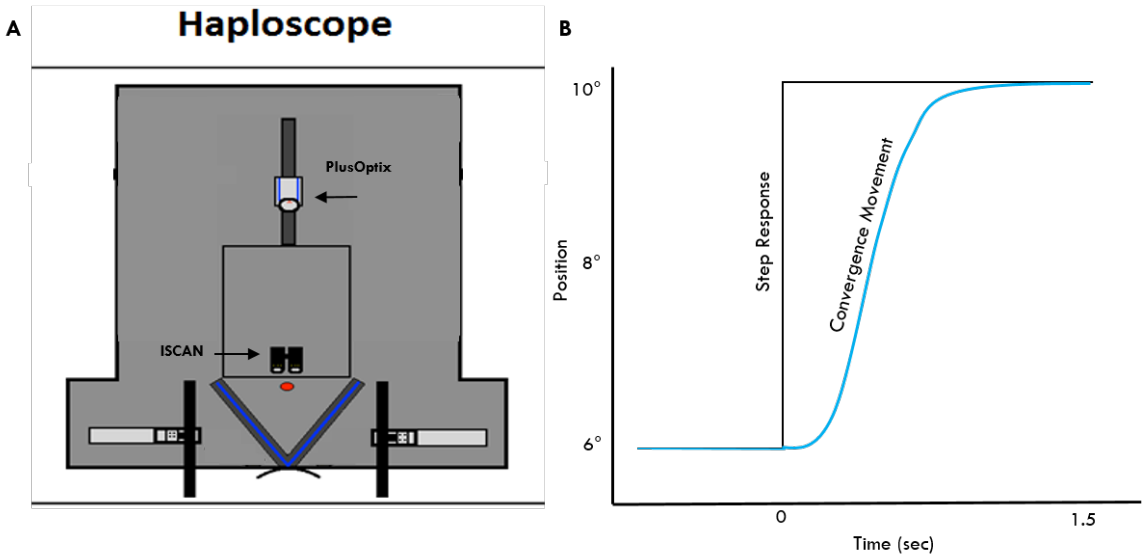

Figure 3.3 A) The haploscope design used to present stimuli in opposing visual fields to subjects and the B) experimental protocol illustrating the presentation of stimulus and vergence movements induced while in the haploscope.

Source: Visualeyes 2020: A Software Suite to Integrate Instrumentation to Study the Near Triad of Vergence. Stephen J. Lestrange. January 2015.

The PlusOptix PowerRef 3® (Figure 3.3A) is used in this study to collect information about the accommodative state of the crystalline lens while engaged in vergence movements. The PlusOptix PowerRef 3® is a photorefraction system that allows us to measure the refractive states of each eye with a sampling rate of 50Hz. The validity of the power refractor to determine refractive states was first described in a laboratory and clinical study (Schaeffel et al. 2000). Since that time, research and clinical labs have conducted validation studies in measuring the refractive states in both human adults (Abrahamsson et al. 2003, Allen et al. 2003, Hunt et al. 2003) and infants (Blade, P.J. and Candy, T.R. 2006).

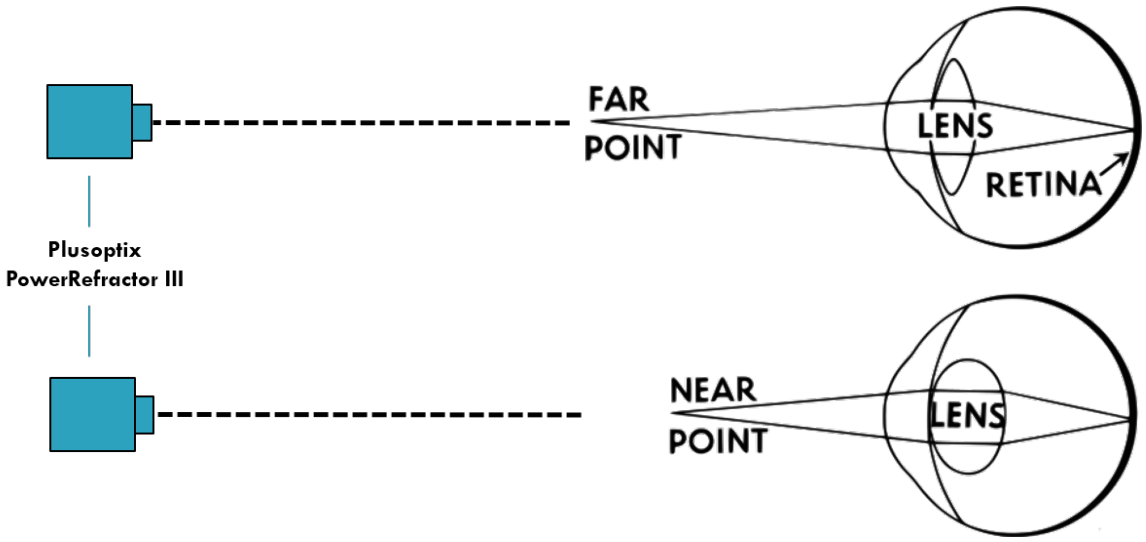

Figure 3.4. Diagram showing the Plusoptix PowerRefractor III setup in order to dynamically capture the accommodative state of the lens during vergence eye movements.

In a recent study, it was shown that photorefraction estimates of the state of the lens is correlated to the ethnic origin of the eye being measured (Sravani NG et al. 2014). To take this into account, we conducted our own plusoptix calibration for every subject that participated in this study (Figure 3.5).

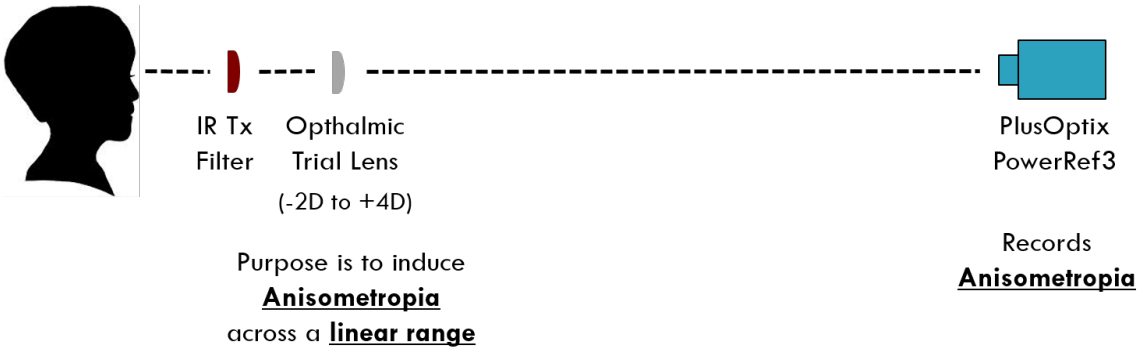

Figure 3.5. Setup of the Plusoptix calibration procedure.

In order to calibrate the system, we look for a linear relationship between a user-defined input to the system as shown in Figure 3.6 and the anisometropia that the PlusOptix records. This is done by occluding one eye with an IR Tx filter where no visible light can pass thru the filter while still allowing the PlusOptix to detect and record IR signal. Then, a convex-sphere trial lens of -2D is placed in front of the occluded eye which will induce a change in the refractive state. In order to establish this change in refraction across a linear range, we use lenses of -2D to +4D.

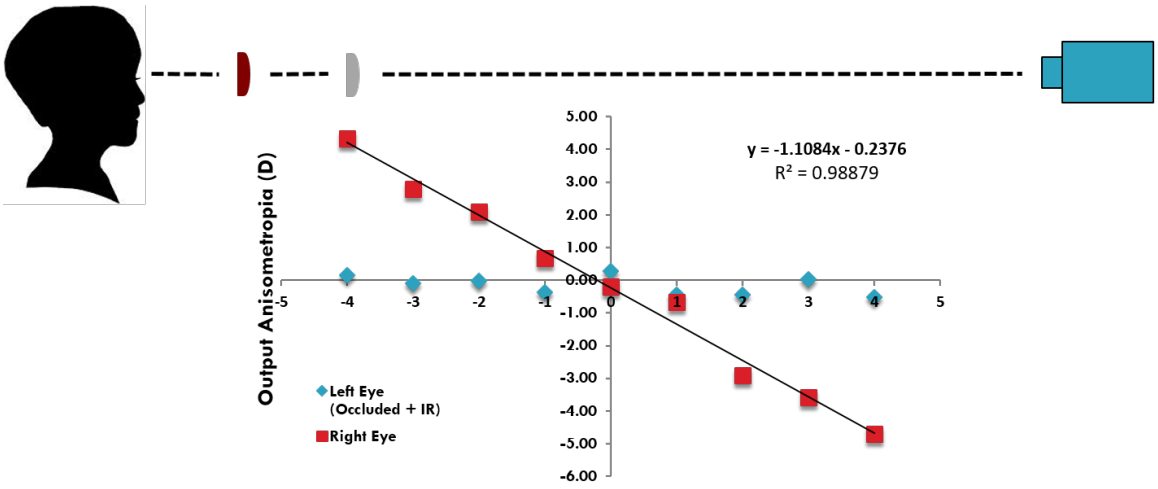

Figure 3.6. Example of a calibration curve recorded for one subject.

Figure 3.3B illustrates the experimental block design. Here, a range of 6° to 10° is used with a binocular pedestal of 8°. The subject begins with a fixation point of 6° binocular and when a trigger is depressed, a convergence movement to 10° is evoked. After the first movement concludes, the subject may rest, or blink if needed before moving on to the next of twelve unique convergence presentations.

In addition to data obtained via eye tracking instrumentation, clinical measures were also taken prior to subjects engaging in the aforementioned trials. To assess motor

preference, a sighting-dominance measure is implemented. Subjects are asked to continually maintain focus on a target while using their hands to slowly create an aperture around the target thus forcing a monocular viewing situation. To assess a sensory preference, or sensitivity, subjects wear a red-green lens while viewing a pen-tip flashlight in a dark setting and are asked to report whether the light appears red or green. These objective measurements are noted from each subject to assess any potential connection to the eye movement metrics obtained as a result of their participation in the study.

Raw data are processed and analyzed using MATLAB scripts. Vergence movements that a) suggest fusion of the monocular stimuli does not occur and/or b) are influenced by saccades during the transient portion of the vergence movement are discarded.

Primary metrics used to assess left and right eye vergence eye movements are peak velocity and latency. Each trial consists of twelve unique observations and two distinct within-subject factors (size and color). As all subjects participated in each trial condition, a repeated-measures ANOVA (rmANOVA) was performed to eliminate individual differences as a source of between-group variability whereby all between-group variability would be due to differences in trial conditions (i.e. stimulus size, color, or a combination of both). There are no individual differences between trials because all subjects undergo the same trials.

3.3 Results

Figure 3.7 shows the effect of stimulus size across all color presentations on both left eye (A) and right eye (B) latency measures. A repeated-measures ANOVA confirmed a significant effect of size on convergence latency $F(2, 28) = 37.468$, $p<.001$.

No effect of color or the interaction between size and color were found with respect to latency. No significant effect was found between size, color, and their interaction with respect to left eye and right eye convergence peak velocities.

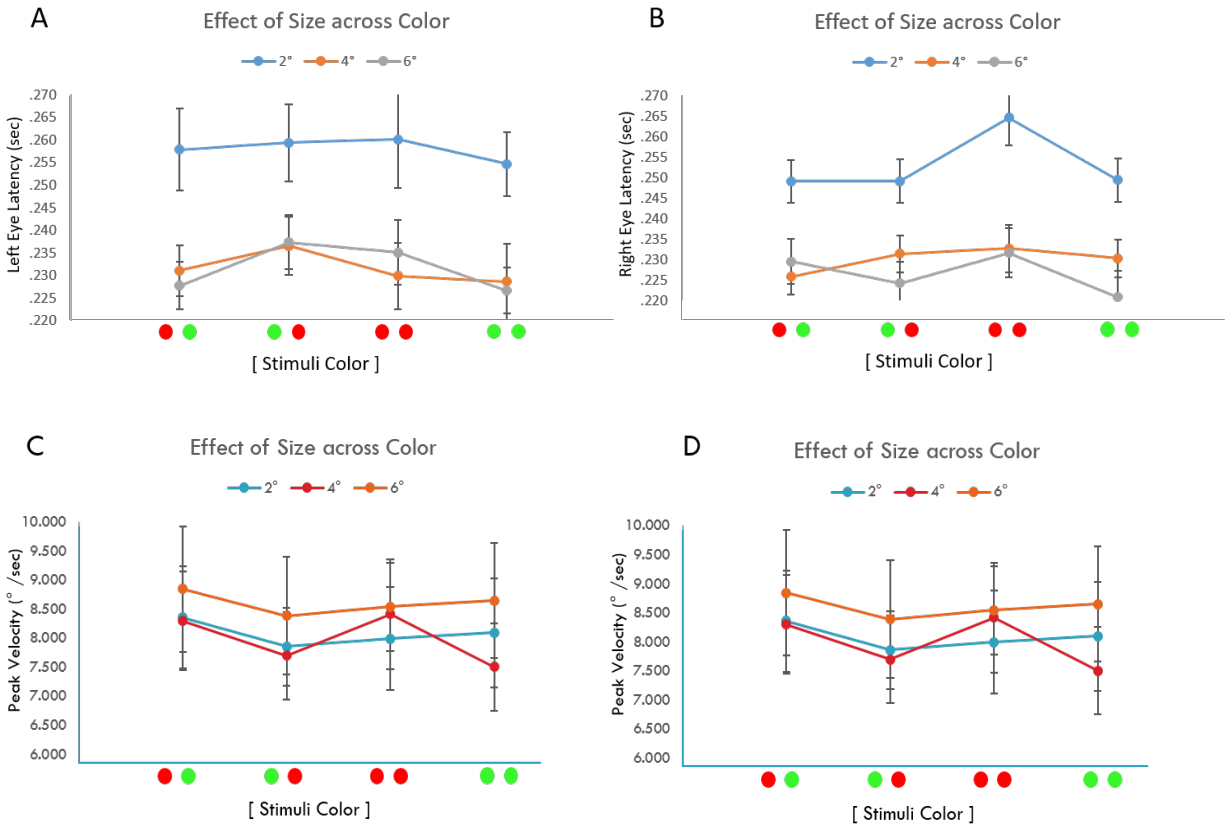

Figure 3.7 The effect of stimulus size across color for (A) the left eye latency and (B) right eye latency along with (C) the left eye peak velocity and (D) right eye peak velocity.

As three different size parings were presented, a post-hoc paired t-test with Bonferroni correction was performed to assess potential differences between left eye and

right eye latencies with respect to target size. A paired t-test of left eye and right eye mean velocities across pairings of all size groups revealed no statistically significant differences ($p \geq .278$). Figure 3.8 is a scatter plot of left eye latency versus right eye latency to illustrate the findings of the paired t-test. Latency pairings across 2° (p=.278), 4° (p=.366), and 6° (p=.206) are plotted along with a reference line (dotted y=x).

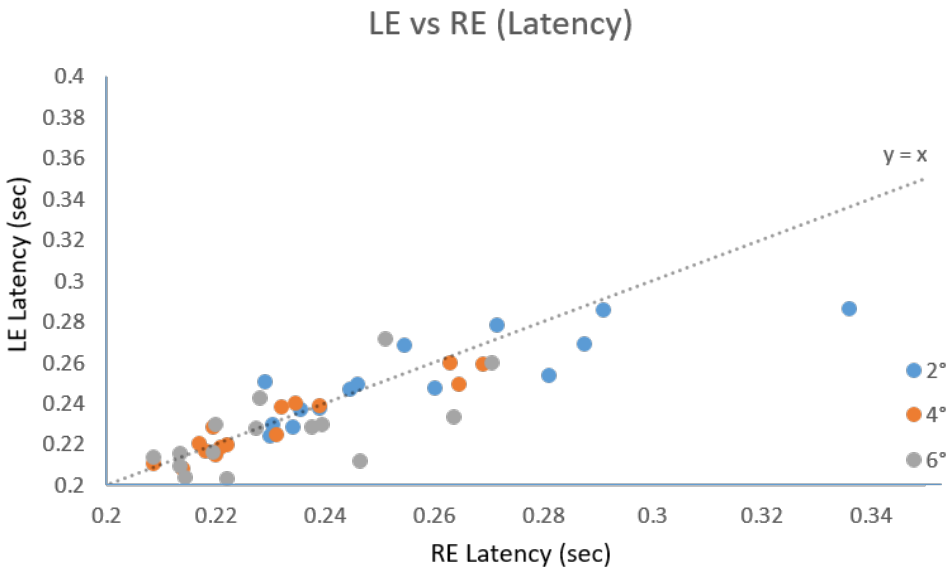

Figure 3.8 The effect of stimulus size across color for (A) the left eye latency and (B) right eye latency.

Figure 3.9 shows convergence eye movement traces across all target sizes for a typical subject. Figure 3.6A1-A2 shows the mean left eye and right eye position trace while viewing the 2° target size where the red line indicates the latency response. Latency was calculated as the time it takes the vergence response to have moved a certain distance from the floor (x-axis) where the distance, or separation from the floor, is calculated with respect to the peak velocity of the vergence response. Compared to the 4° (Figure 3.6B1-B2) and 6° (Figure 3.6C1-C2) responses, the convergence response to the smallest target stimuli (2°) were significantly slower ($p < .001$)

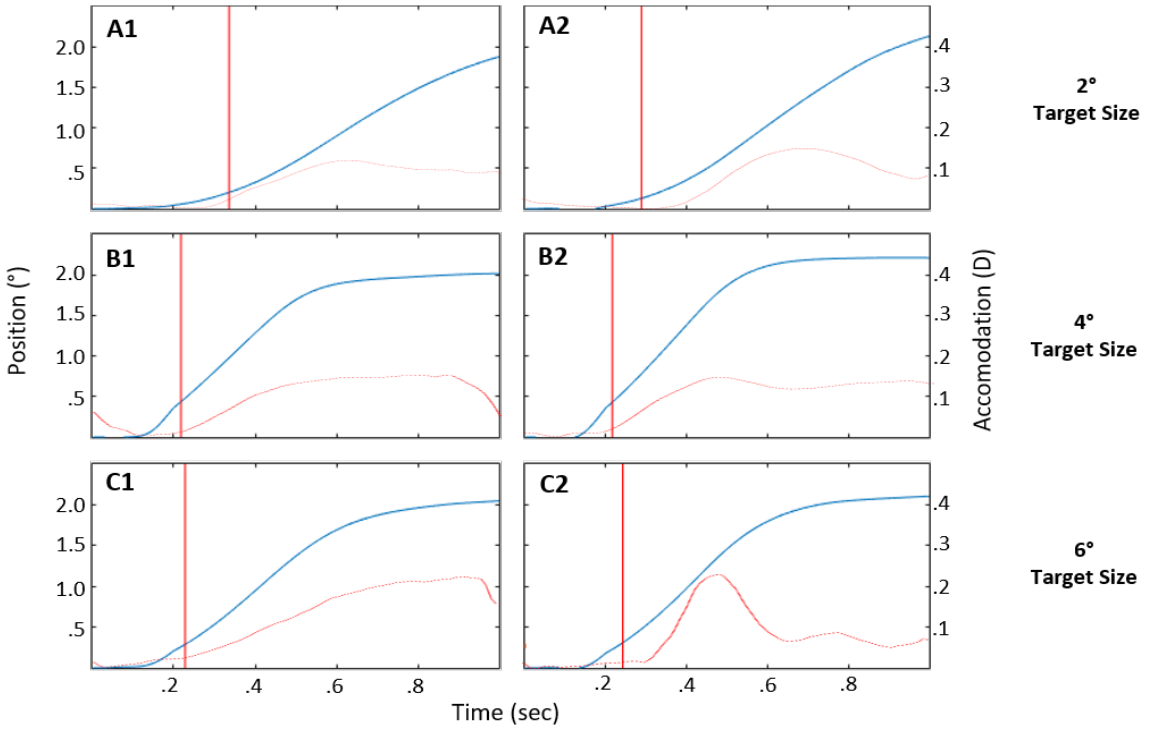

Figure 3.9 Typical Convergence Movement across Size. Position and velocity data from a typical subject. A1 (left eye) and A2 (right eye) show convergence position traces (blue) along with accommodation measures (red) while viewing a 2° target. B1, B2 and C1, C2 depict convergence position traces and accommodation measures while viewing target sizes of 4° and 6°, respectively. The vertical red line demarcates the calculated latency point of the convergence movement.

Latency data are segregated by motor and sensory preferences (See Appendix A). Subject motor and sensory preferences are used to segregate data results in order to test for any effects. Figure 3.10 shows results grouped by subject motor and sensory preferences in a radar plot. The first quadrant indicates subjects with a right eye (R) motor and red sensory (R) preference. Quadrant two is populated with latency measures from subjects that showed a left eye (L) and red sensory (R) preference. Quadrant three displays latency data from subjects with a left eye (L) and green sensory (G) disposition whereas latency measures grouped in quadrant four are from subjects that had a right eye (R) and green sensory (G) preference. Paired t-tests of subject motor and sensory

preferences showed no significant effects on latency and peak velocity measures across all target sizes ($p > .316$).

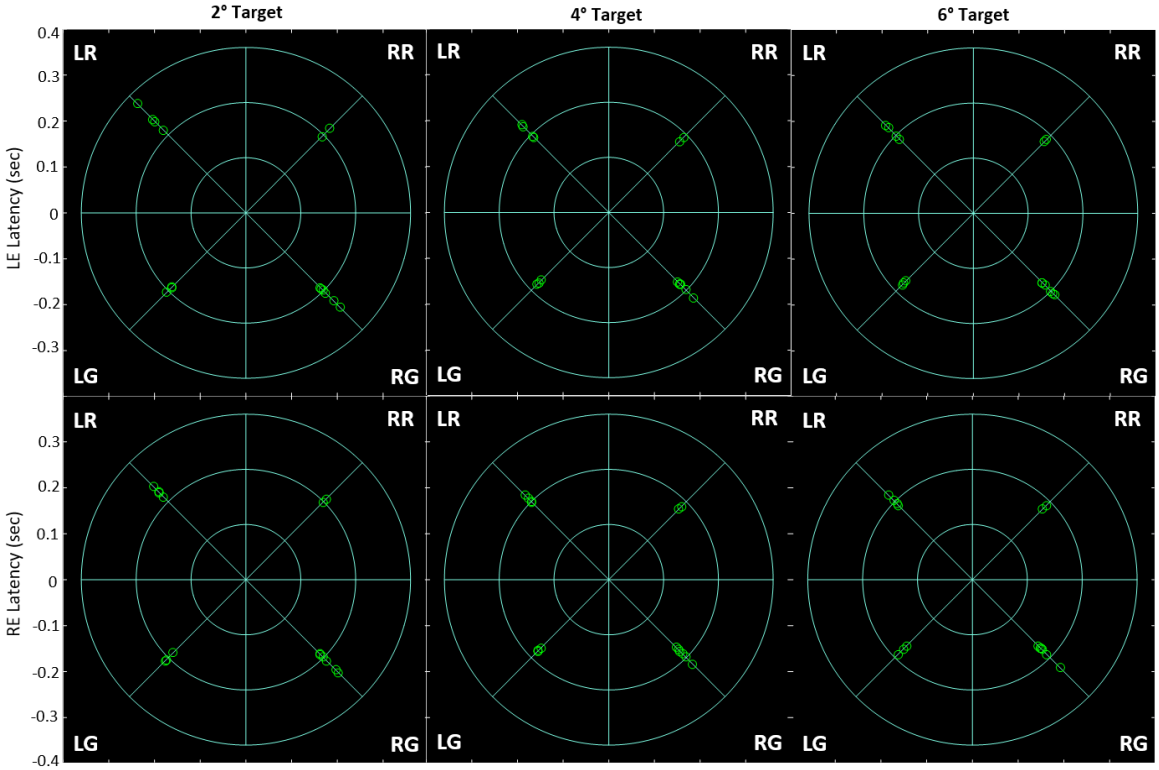

Figure 3.10 Radar Plot where latencies are grouped into quadrants (1: Right/Red, 2: Left/Red, 3: Left/Green, 4: Right/Green) by subject's motor and sensory preferences. Left eye (top) and right eye (bottom) latencies are plotted separately and are charted across stimulus size presentation (left column: 2°, middle: 4°, right: 6°).

Latency data are also separated by subject phoria measurements. Subject phoria measurements are used to isolate data results in order to test for any potential effects on left eye and right eye latency. Figure 3.11 shows results of left eye and right eye latency measures with respect to phoria scores and are grouped by the three possible size presentations. No significant effects on phoria were found on latency across all target sizes ($p > 402$).

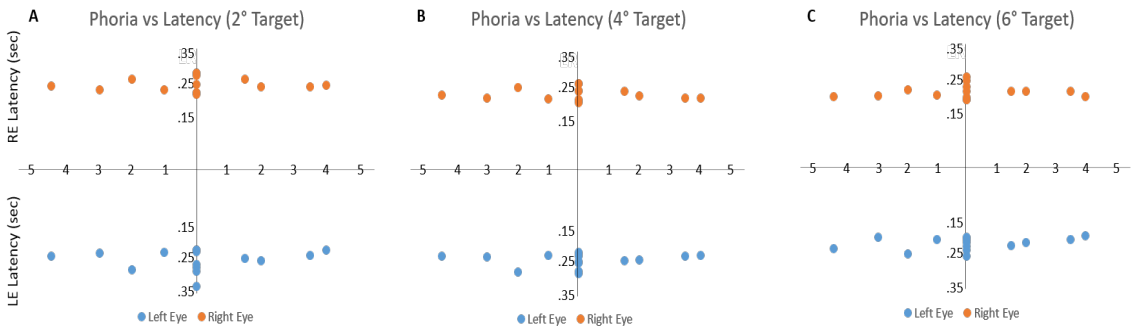

Figure 3.11 Phoria measures vs left eye (top) and right eye (bottom) latencies across varying target sizes (A: 2°, B: 4°, C: 6°).

3.4 Discussion

Eye movements play an integral role in research as they can serve as a vantage point in understanding the neural mechanisms that drive our oculomotor system. A large body of work is readily available investigating eye movements ranging from saccades (Land 1999) and smooth pursuit (Krauzlis 2004) to vergence (Mays et al. 1986, Semmlow et al. 1986). Detailed reviews on eye movements (Kowler 2011, Schutz et al. 2011) are available for reference. Vergence eye movements, in particular, are greatly studied in binocularly healthy controls, subjects with lesions (T. Sander et al. 2009) and those that are afflicted with accommodative (Scheiman et al. 2011) and vergence (TL Alvarez et al. 2010) dysfunction. Comparing the aforementioned subject populations can help us understand behavioral disorders and learning disabilities such as ADHD (Borsting et al. 2005). In addition to corroborating histological findings with research in primates (Ward et al. 2015) and humans (Jaswal et al. 2014), vergence studies provide clinical insight that can assist in developing effective rehabilitative and therapeutic protocols (Scheiman et al. 2015).

Clinicians use targets that range in color and size for vision therapy and clinical measurements. In this study, we investigated vergence eye movements with respect to these two potential contributors to visual target saliency: size and color. Results from this experiment indicate that the size of the stimulus is an important factor when tending to targets in the visual field. Target size has an influence on the response time with respect to the initiation of vergence eye movements. A larger image will stimulate the retina not only centrally but peripherally, beyond the bounds of the fovea centralis. This leads to a decrease in response time and perhaps lower latency measurements while viewing the 4°

and 6° targets may be attributed to an increase in neural recruitment and subsequent innervation of the lateral and medial rectus muscles.

It is important to note that as the size of the target increases beyond the region of the fovea centralis, there is an exponentially diminishing return with respect to the number of cones that are stimulated via light. This may explain why no statistically significant differences were seen between 4° and 6° convergence latency measures.

Furthermore, although target size was found to influence both left eye and right eye latencies, it was shown that it did not influence left eye and right eye latencies differently.

No statistically significant differences were found in vergence peak velocity and latency measures with respect to the four different left eye and right eye color pairings. The contrasts in left eye and right color pairings seemed to play no role in influencing vergence-tracking dynamics. This is in alignment with prior studies, where it has been shown that color discrimination, even in the periphery, may be as strong as in the fovea centralis (Noorlander et al. 1983; Abramov et al. 1991).

During normal vergence-tracking tasks, changes in focal distance influence both the vergence and accommodative systems. While retinal disparity drives the vergence system such that the target images are aligned with the fovea, the accommodative reflex changes the shape of the natural lens in the eye in order to clearly render the target images. As this experiment employs a haploscope, which is capable of rendering a stereoscopic environment, focal cues are effectively minimized. With our experiment, the focal length is kept relatively constant and thus the accommodative state is expected to not vary substantially. In other words, the subject's distance from the screen which

should remain fixed, will also determine the accommodative stimulus. Our data show that while the vergence-tracking stimulus changed, the accommodative stimulus remained relatively unchanged. Prior studies have shown similar results where the accommodative reflex did not experience change while the vergence stimulus changed in a stereoscopic setting (Joohwan et al. 2014).

Phoria measurements of each subject were recorded prior to the start of vergence-tracking experimental trials to investigate whether the resting position of the eye played a role in vergence dynamics. As differences in latencies were found across stimulus size presentations, phoria as an influencing factor was mapped with respect to left eye and right eye latency measures. No significant differences were found between phoria levels and left eye or right eye latencies across the three stimulus size presentations.

Measurements of motor and sensory preferences were noted prior to the start of the experimental trials. Latency and peak velocity data were grouped by motor and sensory preferences across subjects in order to investigate any potential relation between clinical and convergence responses. No significant differences were found between groups which suggests that motor and sensory preferences do not influence convergence movements.

Without a true cone mosaic image of each subject's retina, it is difficult to objectively assess the left and right eye sensory dominance. Much research is being conducted in this regard where cone mosaic groupings are studied for clumps of (M) and (L) cones or whether these cones are randomly scattered across the central regions of the retina.

As virtual reality (VR) and augmented reality (AR) technology become ubiquitous and widely accessible, studying stereoscopic targets and the vergence responses required to track them become even more important. More insight about vergence eye movement dynamics can be carefully studied in virtual environments where, similar to the haploscope environment, the accommodative demand is held relatively constant. As robust and reliable as a haploscope design is, where many vision experiments can be performed, the oculus can replicate most, if not all, of those same experimental designs with a fraction of the space requirements. With head-mounted displays (HMD) such as the Oculus Rift, Samsung Gear VR, or Valve's HTC Vive, head motion is taken into account and is significantly reduced as a potential confounding variable.

3.5 Conclusion

Data from this study shows that stereoscopic target color does not influence vergence peak velocity and latency across both the left eye and right eye. However, stereoscopic target size significantly affects both the left eye and right eye latency during convergence eye movements. Accommodative levels of both left eye and right eye were found to not significantly vary between each of the twelve unique target presentations. Furthermore, the left eye and right eye latencies do not significantly differ across target sizes ranging from 2°, 4°, and 6°. In addition, motor and sensory preferences along with baseline phoria levels did not have a significant effect on the left eye and right latency across all target sizes.

CHAPTER 4

REPEATABILITY OF VERGENCE TASKS IN FMRI

4.1 Background and Significance

While conjugate eye-movements such as saccades (Kimmig et al. 2001, Luna et al. 1998) and smooth-pursuit eye movements (Nagel et al. 2004, Petit et al. 1999) have been studied extensively using fMRI, vergence eye movements have not been as thoroughly investigated with fMRI. Vergence eye movements allow for stereoscopic vision by rendering parametrically offset visual inputs of the same visual scene from two eyes into one three-dimensional scene. As opposed to saccades and smooth-pursuit, they are disconjugate eye movements that are meant to facilitate the tracking of objects at varying distances (near compared to far space). As such, vergence experimental tasks involving functional MRI (fMRI) are readily primed for investigation. In prior studies, the human vergence system has been studied in conjunction with fMRI to delineate vergence neural substrates (Jaswal et al. 2014), correlate functional cortical activity to behavioral data (Alvarez et al. 2014) as well as to study cortical vergence networks in primates (Ward et al. 2015).

Functional MRI investigations have the potential to produce data that can shed light on vergence-related neural networks and also corroborate prior clinical (Scheiman et al. 2005) and primate findings (Gamlin et al. 2000, Gamlin et al. 2002) on the control mechanisms of the vergence networks. With the widespread use of functional magnetic resonance imaging (fMRI) in research, the human oculomotor system can be non-invasively studied to investigate cortical areas involved in processing visual information.

It stands to reason, then, that the reproducibility of results obtained via functional MRI should be ratified to lend confidence to prior, current and future studies that focus on fMRI and vergence eye movements.

In a prior study (Kimmig et al. 2001), the pattern of saccadic eye movements and its relationship to the corresponding BOLD signal were investigated and showed that the frequency of saccadic stimuli presentation were correlated to the BOLD signal. To our knowledge, a similar study in vergence eye movements has not been conducted. Moreover, functional activity is investigated by analyzing spatial activation and percent signal change within ROIs during vergence tasks where frequency of eye movements varied between a slow and fast presentation. Specifically, this study is designed to investigate frequency of a vergence task to the corresponding blood oxygenation level dependent (BOLD) signal.

This study investigates the functional activity and task-modulated coactivation of the neural networks used to generate a vergence eye movement. The following aims were tested: 1a) Assess the intraclass correlation for same day sessions of the same trial. 1b) Assess the interclass correlation for between-day sessions of the same trial. 2) Assess the efficacy of an updated experimental block design with respect to percent signal change of the BOLD signal. 3) Asses the efficacy of an updated experimental block design with respect to task-based coactivation.

4.2 Research Design

Seventeen subjects (12 male, 5 female) participated in this study. All subjects had no history of binocular dysfunction and were between the ages of 18 and 35 years. Normal binocular vision was defined as having a normal near point of convergence (NPC) less than 6cm, which was assessed by measuring the distance a high acuity target, was perceived as diplopic along the subject's midline (Von Noordern GK and EC Campos 2002) and a normal stereopsis (≤ 50 seconds of arc), assessed by the Randot Stereopsis Test (Bernell Corp., South Bend, IN, USA). All subjects signed written informed consent forms approved by the New Jersey Institute of Technology (NJIT) Institution Review Board (IRB).

A 3-Tesla Siemens Magnetom TrioTim scanner with a 12-channel head coil was used to perform the fMRI scans. The fMRI imaging protocol used during the scans consisted of the following parameters: time of repetition (TR) = 2000 ms, time of echo (TE) = 13ms, field of view (FOV) = 192mm, and flip angle = 90 degrees. A total of 53 slices were collected (axial orientation) with a slice thickness of 3.0 mm. The voxel resolution was set to 3.0 x 3.0 x 3.0 mm3. High resolution anatomical volumes acquired using a magnetization-prepared rapid acquisition with gradient echo (MPRAGE) were collected in addition to functional tasks as a part of the imaging protocol. The MPRAGE imaging protocol consisted of the following parameters: TR = 1900 ms, TE = 2.52 ms, T1 = 900 ms, with a total of 176 acquired slices. The voxel resolution was 1.0x1.0x1.0 mm3. Subjects were instructed to limit head motion and foam wedges were placed around head to facilitate the restriction of physical movement inside the head-coil. All subjects were comfortably positioned supine on the gantry of the scanner and were

instructed on how to align their heads along the midline of the coil to ensure symmetrical vergence step stimuli were observed.

A single-camera Eyelink 1000 with a sampling rate of 1000Hz was used to collect eye movements and track the right eye pupil to ensure subjects performed vergence eye movements during the vergence tasks.

The visual stimuli used during the vergence tasks consisted of simultaneous vergence targets (Figure 4.1C). The visual stimuli were designed to facilitate subjects in achieving fusion of the targets. This stimuli is important because different amounts of retinal disparity are presented so that the subject has the perception of the inner most box being closest to the subject and the outer most box appearing furthest away. Subjects were instructed to view the visual targets via a mirror, carefully attached to and positioned along the midline of the head coil. The experiment utilized (Figure 4.1B) a block design that consisted of three states: 1) Rest for 16s, 2) Slow Vergence for 24s, and 3) Fast Vergence for 24s. Slow vergence is defined as 4 vergence stimuli presented within the 24s and Fast Vergence is defined as 10 vergence stimuli presented within the 24s. As prediction has been shown to decrease the latency and peak vergence velocity of convergence responses (Alvarez et al., 2002, 2005, 2010a; Kumar et al., 2002a, 2002b), this experiment utilized random delays prior to stimuli presentation to reduce anticipatory or predictive cues.

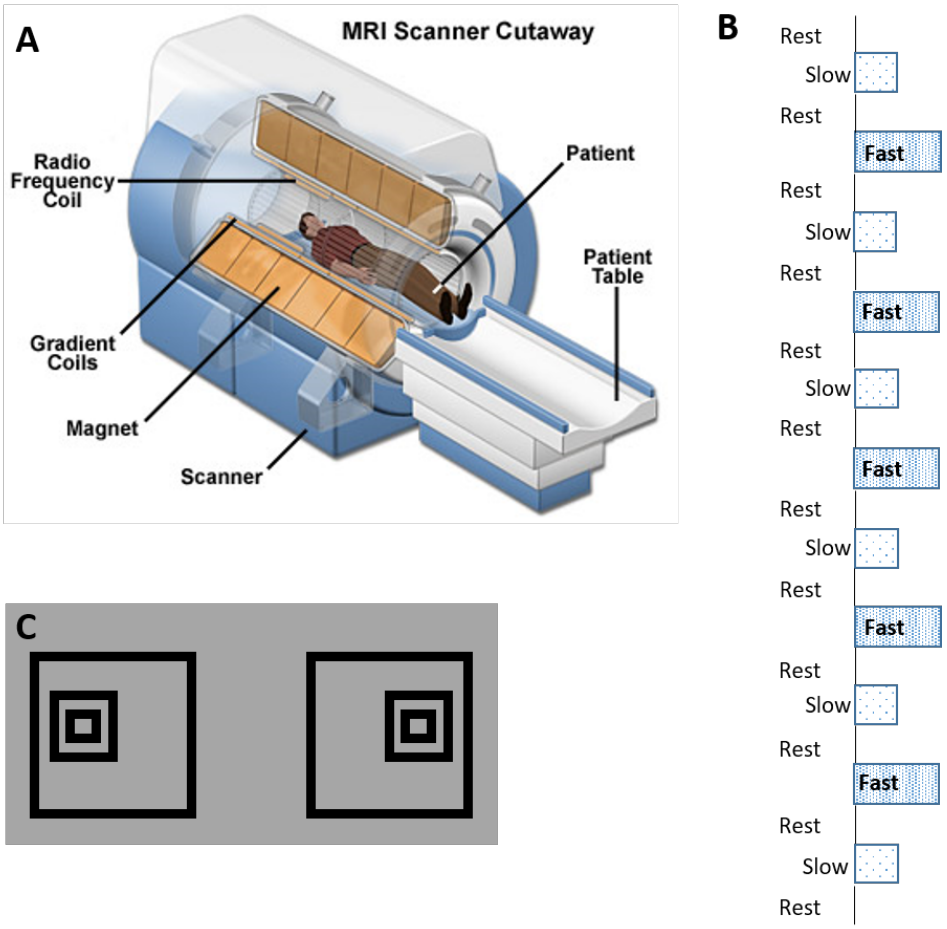

Figure 4.1 A) Subject lays supine on the gantry of the scanner while viewing targets via mirror attached to 12-channel head coil. B) Experimental block design used during vergence eye movement tasks consisting of 3 conditions (rest, slow, fast) C) An example of the third-degree visual stimuli used in order to facilitate voluntary vergence eye movements.

Source: Figure 4.1A. http://4.bp.blogspot.com/mri-scanner.jpg.

During the vergence task, subjects engage in a total of 11 rest blocks, 5 slow vergence blocks, and 5 fast vergence blocks. Rest blocks have a duration of 16 seconds where both slow and fast vergence blocks have a duration of 24 seconds. As timing of the task is paramount to the applied BOLD sequence, each task is pseudorandomized to remove the subject's ability to anticipate vergence movements while ensuring subjects are exposed to the same number of vergence movements during each slow block and each fast block. Slow blocks consist of a total of 4 vergence movements while fast blocks

induce 10 vergence eye movements. During the rest block, the vergence angle is set to 4° and during the slow and vergence blocks, vergence angles range from a position of 1° to 7° where vergence movements in this range occurs at steps of 2° to 4°.

MR Data were processed and analyzed using a suite of software tools. SPM12 (Friston et al. 2001, Wellcome Trust Centre for Neuroimaging) was utilized for spatial preprocessing of raw MR data obtained from the scanner (Figure 4.1A). Preprocessing included the following steps: 1) Motion Correction, 2) Co-registration, 3) Segmentation, 4) Normalization and 5) Image Smoothing. Spatial preprocessing is the most straightforward part of SPM analysis. During this phase, images are aligned with each other, normalized such that each subject's anatomy is relatively the same shape, corrected for differences in slice time acquisition, and spatially smoothed.

After smoothed images are created, level-1 General Linear Model (GLM) analysis at the subject level is performed using SPM12 where the first 5 time points are removed to mitigate scanner artifact. This step involves experimental design creation and model estimation where task parameters are included along with 6 motion regressors (x, y, z, roll, pitch, and yaw).

Model estimation lies at the core of the SPM software package. As we defined all parameters pertaining to the fMRI experiment we therefore have a list of the different conditions and at what times each of them transpired. Our model of the person's brain is that there was some reaction in the brain for every stimulus that occurred. What we seek then are particular locations in the brain where our model was a very good fit, and others where it wasn't a good fit. SPM allows us to locate these areas. This is important because

locations where your hypothesis proves to be a good fit can be described as "responding" to the conditions in our experiment.

With model estimation in SPM, a rather large multiple regression at each voxel of each subject's brain is being performed to see how well the data across the experiment fits the hypothesis, which is created in SPM as a design matrix. Our design matrix contains our experimental information such as conditions, their onset vectors, filters, etc. SPM automatically convolves the effects of the hemodynamic response function with our stimulus vectors. With our design matrix finalized, SPM will conduct a multiple regression through every voxel in the brain and estimates how large of a contribution each specified condition in our experiment made to the data and how much error was left over after all conditions are taken into account. A large positive or negative partial regression slope for either condition signifies that condition had a large influence in determining the data at that specific voxel. This slope information, or beta weight, is saved by SPM; one for each column of the design matrix, where each voxel gives the beta weight for that condition at that point.

Immediately after design files are created for each subject task, contrasts are then created to differentiate between the three distinct states of our block design (A - Rest, B - Slow Vergence, C- Fast Vergence). Composite contrasts were created where subtractions between the slow and fast tasks could be investigated (e.g., Fast minus Slow or Slow minus Fast). SPM asks for a contrast specification in terms of weights for each condition (e.g., slow or fast). Since we used two primary conditions for this experiment (see Figure 4.4: columns 1 and 2 from our design matrix), we were able to make contrast vectors of [0 1], [1 0], or [-1 1]. The contrast vector [0 1] denotes at which voxels the “fast”

condition had a significant contribution to brain activity. The contrast vector [1 0] denotes at which voxels the "slow" condition had a significant contribution to brain activity. The contrast vector [-1 1] denotes at which voxels the "fast" condition had a significantly larger contribution to brain activity than the "slow" condition did. SPM takes the contrast vectors and uses it to make a weighted sum of the beta images calculated during the level-1, or subject-level, analysis.

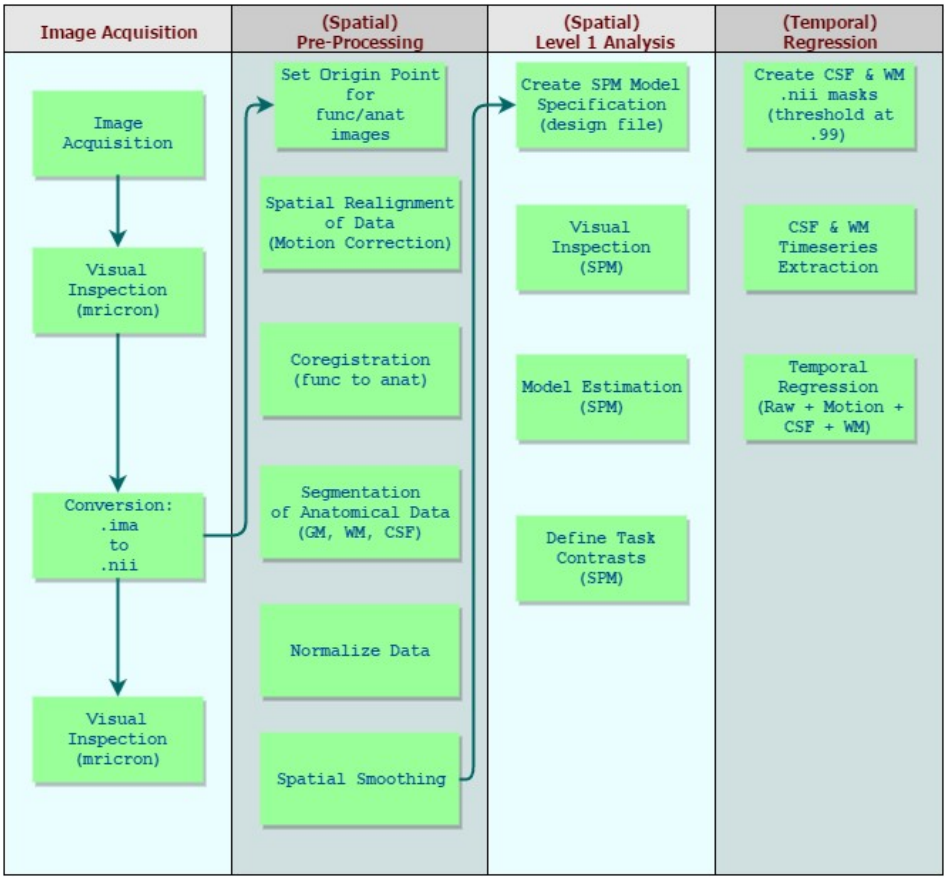

Figure 4.2 Data processing steps used to analyze raw data from the MR Scanner.

Immediately following subject-level spatial processing is the group-level analysis. Groups are categorized based on session (Session 1 or Session 2) and task (Vergence Task 1 or Vergence Task 2). Such grouping allows for analysis within sessions and between sessions with respect to the vergence tasks. Furthermore, as contrasts are used to

suppress the BOLD signal from the slow and fast blocks of the vergence task, comparisons can also be made with respect to the differences in vergence frequency.

Eyelink Data were processed using a custom-built VNEL program, EDFAnalyzer. This program takes raw data from the SR Eyelink 1000 system at the end of a recording session and converts it to calibrated eye movement position traces. These position traces ensure us that the subject is able to perform the vergence movement or attempting to make the vergence movement.

In addition to saccades, the frontal eye field (Yang et al. 2011, Gamlin et al. 2000, Ferraina et al. 2000) the posterior parietal cortex (Kapoula et al. 2005) and the primary visual cortex (Cumming et al. 2001, Masson et al. 2001) have been shown to be involved in the initiation of vergence eye movements. Figure 4.3 shows the ROIs investigated in this study.

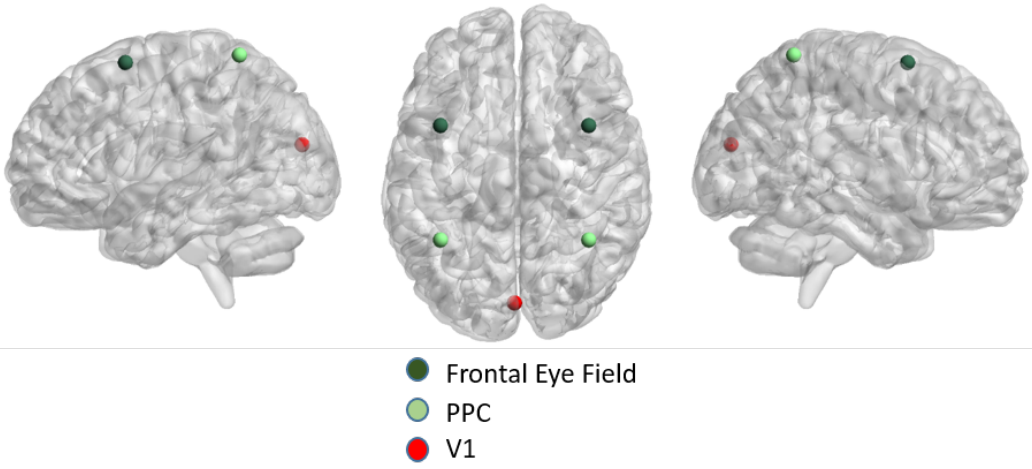

Figure 4.3 Data processing steps used to analyze raw data from the MR Scanner.

4.3 Results

Figure 4.5 shows the group-level spatial activation seen during the slow (B1, B2) and fast (A1, A2) blocks of the vergence tracking task. Statistical significance is reached at $T \geq 3.134$ ($p < .05$). Two primary contrasts were used in SPM (Figure 4.4) to isolate the effect of the slow vergence and fast vergence tracking task with respect to induced blood flow. A one-sample t-test (Figure 4.5: A1, A2, B1, B2) is used to illustrate the areas involved in the frequency modulated vergence tracking task. As can been seen in Figure 4.5A1 and Figure 4.5A2, the fast vergence tracking task induces considerable spatial activation in vergence-related network areas as compared to the slow vergence tracking task seen in Figure 4.5B1 and Figure 4.5B2. Further, a paired t-test is performed to make comparisons between sessions for both the slow vergence and fast vergence tracking tasks. No significant differences are seen between sessions in vergence-related ROIs during both the fast (Figure 4.5A3) and slow (Figure 4.5B3) tasks.

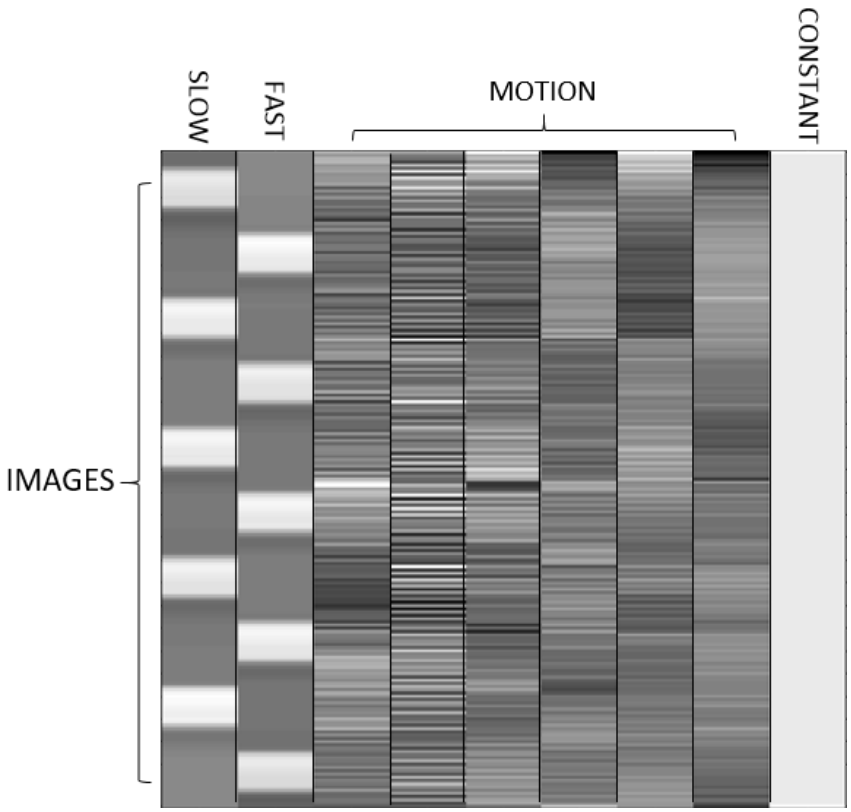

Figure 4.4 An SPM design contrast file showing the slow and fast contrasts used.

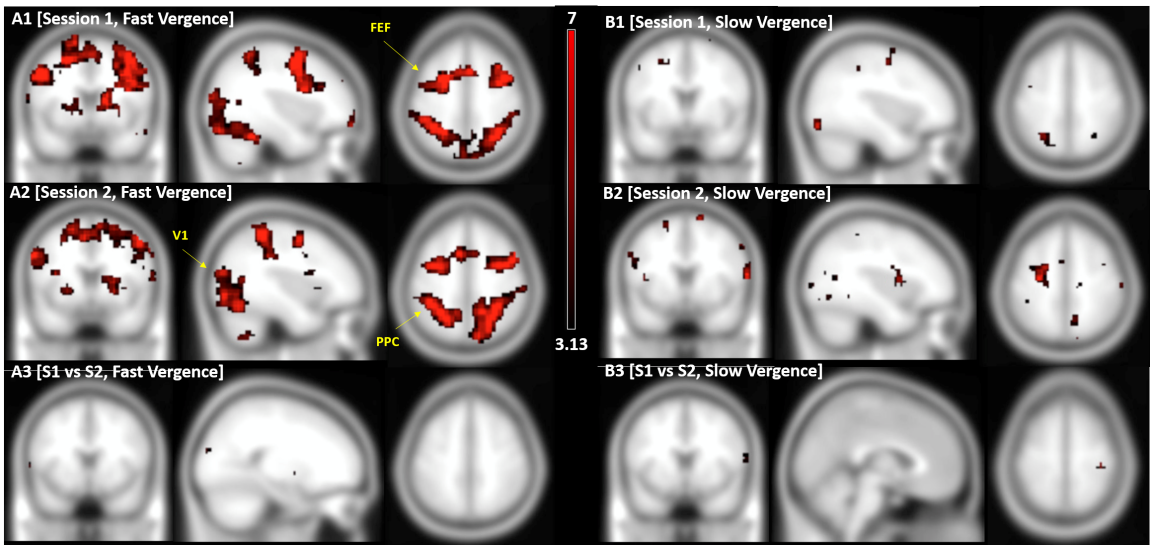

Figure 4.5 Group-level spatial activation maps. A1) Session 1 Fast Vergence. A2) Session 2 Fast Vergence. A3) Session 1 Fast Vergence vs Session 2 Fast Vergence via paired T-Test. B1) Session 1 Slow Vergence. B2) Session 2 Slow Vergence. B3) Session 1 vs Session 2 Slow vergence via paired t-test.

Figure 4.6 shows maps of the whole-brain interclass (between sessions) and intraclass (within session) correlation coefficients across the slow and fast vergence tracking task. Figure 4.6A1 and Figure 4.6A2 shows the between session correlation for the slow and fast task, respectively. Figure 4.6B1 and Figure 4.6B2 shows the within session correlation for the slow and fast task, respectively. Vergence-related ROIs show high correlation (≥ 0.5) for intersession and intrasession comparisons of the slow and fast vergence-tracking tasks.

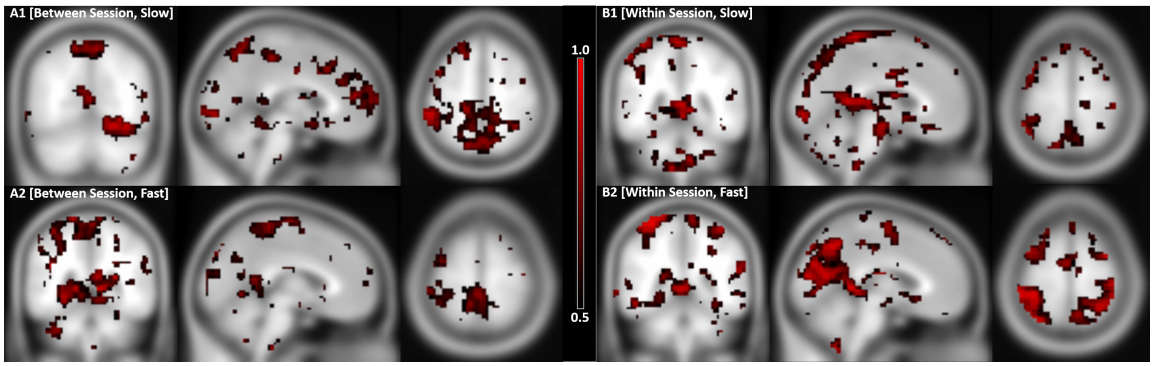

Figure 4.6 Group-level ICC maps. A1) Intersession VM1 Slow. A2) Intersession VM1 Fast. B1) Intrasession VM1 Slow. B2) Intrasession VM1 Fast.

A total of five ROIs were investigated in this study. Frontal eye fields (left and right), posterior parietal cortex (left and right) and the primary visual cortex. Figure 4.7 illustrates the mean percent signal change in the raw BOLD MR signal across these ROIs for all subjects. The BOLD percent signal change for each ROI per subject comparing elevated activation observed during the vergence task to the baseline of sustained fixation was computed from the raw time series. The individual-subject percent signal change values were pooled to conduct the group-level comparison show in Figure 4.7.

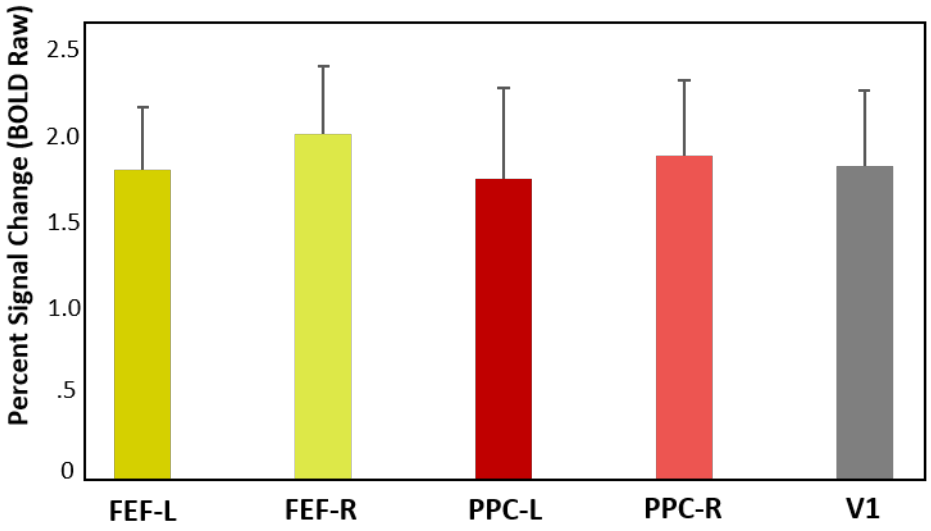

Figure 4.7 Mean percent signal change across ROIs (Frontal Eye Field, Posterior Parietal Cortex, and V1).

Figure 4.8 highlights the effect of vergence tracking frequency on the raw BOLD signal across ROIs. Here, the BOLD signal for each ROI per subject comparing elevation activation observed during the active vergence tasks to the baseline of sustained vergence fixation was computed from the regressed time series. Statistically significant differences were consistently found between the rest and fast vergence state ($p<.001$) as well as the slow vergence and fast vergence state ($p=.002$). No differences were found between the rest and the slow state ($p>.191$).

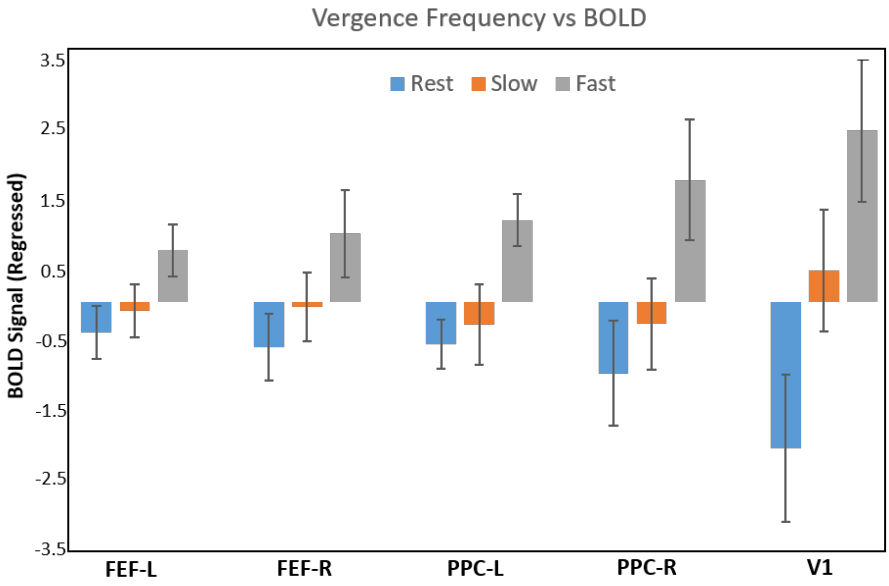

Figure 4.8 BOLD signal during each of the three task states (rest, slow, fast) across regions of interest.

Regressed timeseries were used to investigate the temporal relationship of ROIs between sessions. Figure 4.9 shows correlation maps of the vergence network ROIs between session 1 and session 2 where Broca's region served as a control ROI (not related to the vergence network model). Most regions were able to maintain strong correlation during both sessions 1. However, there seems to be a slight decrease in the correlation between the frontal eye field and the primary visual cortex during session 2.

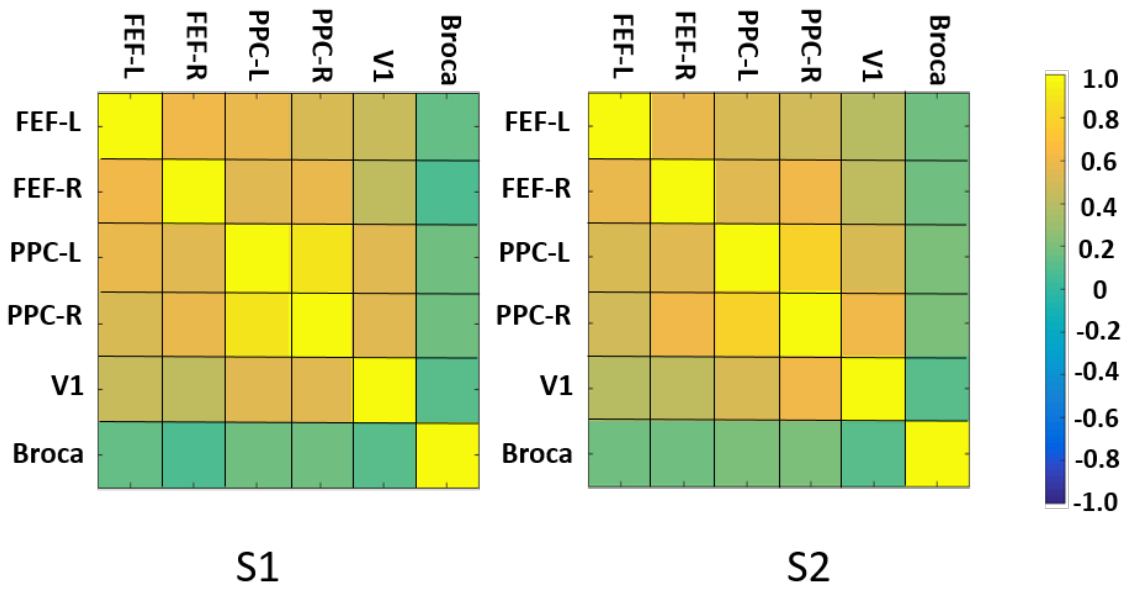

Figure 4.9 Pairwise correlation. Group-level correlation is investigated for ROIs (FEF-L, FEF-R, PPC-L, PPC-R, and V1) between session 1 and session 2.

To ensure task compliance for eye movement tasks during fMRI, right eye movements were recorded. Figure 4.10B shows a typical eye movement response during a slow vergence-tracking task while figure 4.10C shows a typical eye movement response during a fast vergence-tracking task.

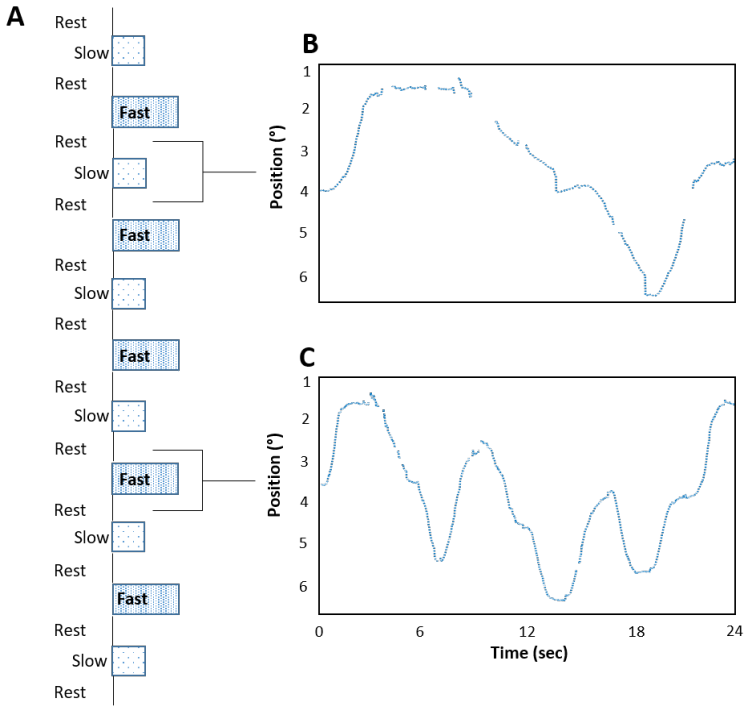

Figure 4.10 Eye movements for a typical subject during A) slow and B) fast vergence tracking fMRI tasks.

4.4 Discussion

With the recent influx of imaging and eye movement publications, the broad applications and practicality of functional MRI is evident. As prior studies have shown, MRI has established itself as a mainstay investigative tool to non-invasively study eye movements in general. Researchers seek to answer questions regarding the neural substrates involved in driving eye movements from a variety of aspects. From normal functional activation in controls (Petit et al. 2009; Jastorff et al. 2016; Vernet et al. 2014) and subjects with oculomotor deficits due to lesions (Tyler et al. 2015), dysfunctions (Alvarez et al. 2010) and anatomical studies (Clark et al. 2016) to functional co-activation (Jaswal et al. 2014), the functional imaging modality has allowed researchers to non-invasively investigate the healthy oculomotor system that, in the not-so-distant past, was much more difficult to study in humans. In addition, functional MRI provides researchers with information from specific voxels to whole-brain networks. As it stands, more research in the field of vision science, and specifically vergence eye movements, can be done in conjunction with functional magnetic resonance imaging, which reinforces the need for confidence in functional MRI as a viable utility.

We used fMRI as our primary tool to investigate the vergence-related cortical networks involved in vergence tracking eye movements in healthy human subjects. As was the case, the ability to acquire full-scale functional maps of the human cortex during the performance of vergence movements allowed for a fairly accurate mapping of the cortical areas involved, from the frontal eye field and posterior parietal cortex to the primary visual cortex. These maps serve a dual purpose: 1) to apply the general liner model (GLM) at a whole-brain (spatial) level and 2) to apply the GLM at a temporal level

to investigate changes in the BOLD signal timeseries with respect to the aforementioned ROIs.

Both lines of analyses were important in understanding not only the reliability of fMRI with respect to our experimental vergence-tracking tasks, but also to the precision with which the vergence-tracking task design induces a detectable and serviceable hemodynamic response.

As fMRI vergence studies become more prominent, the reliability and repeatability of the BOLD signal should be well documented. Our data indicate a reliable correlation between identical vergence tasks performed not only on the same day, but as well as on different days. Cortical regions involved in vergence eye movements showed high correlation during vergence-tracking tasks within and between sessions.

While it is well established that eye movements influence the BOLD signal (Beauchamp 2003, Tregellas et al. 2002, Kimmig et al. 1999), our experimental design sought to address the effect of frequency modulation of vergence-tracking movements performed during a given task. In 2001, Kimmig and colleagues demonstrated that BOLD responses in ROIs involved in saccadic eye movements were correlated with frequency of the saccade task.

Previously, our vergence-tracking protocols consisted of a block design with two conditions, rest and active. For this study, we used three conditions with two active states: rest, slow, and fast. Our fMRI BOLD signal findings shows a relationship between frequency of vergence activity and cortical activity, as measured by fMRI, within sites linked to the initiation of vergence eye movements (i.e., left and right frontal eye fields, left and right posterior parietal cortex, and primary visual cortex).

Although we were able to show a high interclass and intraclass correlation across vergence related ROIs, it should be noted that while comparing vergence movements to a vergence fixation task, a stronger BOLD response was induced with the faster vergence tracking task, indicating that the continual neural processing of the vergence-tracking eye movements led to a stronger BOLD response. These findings are apparent in spatial activation maps shown at the group level and become quite evident as timeseries analysis is performed at the group level.

While the BOLD signal corresponding to vergence tasks are repeatable within sessions and between sessions, vergence tasks should be designed such that subjects are performing a movement every 2 seconds within a task block to ensure adequate change in the hemodynamic response and subsequently MR signal.

The underlying significance of this research lies in the confidence it lends to long-term studies that would aim to investigate potential changes in vergence neural substrates. Comprehensive longitudinal studies that seek to understand the mechanisms driving vergence movements along with vision rehabilitation stand to directly benefit from our findings as observable changes in the BOLD signal, whether temporal or spatial, can now be reliably corroborated to experimentally controlled independent variables such as applied therapy.

Concussions are the most common type of traumatic brain injury (TBI) and can have lingering effects on a number of cognitive processes (Stone J. et al. 2015). Researchers seek to establish biomarkers that have the potential to reliably deliver initial diagnoses of concussion using resting-state fMRI (Zhu DC et al. 2015) and eye movements (Ventura RE et al. 2016, Maruta et al. 2014)

While it has been shown in prior studies (Jaswal et al. 2014, Alvarez et al. 2014) that those with CI showed an increase in vergence-network connectivity after vision training, more work can be done in understanding connectivity in those that have sustained concussion.

Vision is a high brain level activity, intimately linked to cognition. Most vision impairment (or blindness) is almost always caused by damage to the eyes, visual tracts, or the occipital lobe. As complex as visual processing is at the level of the retina, along the tracts and in the visual cortex, what the brain does at these early levels of visual processing is establish that a visual pattern or contrast exists. Higher-level intelligence is generally unaffected by what is called "vision" impairment and blindness. This is really "sight" or "sensory" impairment. As visual cognition is widespread throughout the brain and occurs beyond the occipital lobe, the effect of visual sensory input and cognition is an important factor to consider in how subjects respond to the vergence-tracking tasks.

4.5 Conclusion

Data from this study has shown clear evidence of between-subject and within-subject reliability when employing vergence-tracking tasks in conjunction with functional magnetic resonance imaging. Furthermore, this study investigated a vergence-tracking protocol with respect to the frequency of induced vergence movements and concludes that a faster vergence-tracking task is associated with a statistically significant increase in the BOLD signal as compared to the BOLD signal derived from the slow vergence task and sustained vergence fixation task.

CHAPTER 5

THE BENEFITS OF A MULTIMODAL APPROACH

Our connectivity project sought to establish the procedures to determine efficacy of vision therapy on subjects with convergence insufficiency by way of an fMRI analysis. In the process, baseline parameters for an experimental vergence-tracking protocol were also established. Percent signal change of vergence-related ROIs (Gamlin et al. 2002) and the connectivity between these ROIs were the main course of the investigation. We were able to show the involvement of cortical vergence-related ROIs with respect to our vergence task.

Now, based on the vergence ROIs studied in the connectivity project we were able to elicit a baseline effect or BOLD response from our vergence tracking task. In an attempt to strengthen this response in future projects, improvements were made to the experimental task design. One important area of improvement focused on a stimuli redesign that would have the potential to serve as a stronger cue for vergence movement.

The asymmetry project played a vital role in understanding the effects of varying stimulus design, not just in terms of size and color, but as well as how they are presented. 2nd degree fusion targets represent the combination or flat fusion of the two foveal images into a single percept whereas 3rd degree fusion targets allow subjects to derive a three dimensional depth perception, or stereopsis. While prior vergence studies have traditionally used 2nd degree fusion targets, we elected for and designed 3rd degree fusion targets in order to facilitate the stereoscopic experience in the haploscope. Positive subject feedback from the 3rd degree stimulus design employed in the asymmetry project

prompted a similar stimulus set to be utilized for the next fMRI project. While adding to the current knowledge for vision tasks carried out in a haploscope, we also were able to corroborate clinical practices of vergence therapy. For example, as subjects with CI first undergo vergence training, clinicians usually have them start with targets that are much larger and thus, easier to fuse. This is in alignment with the response times our subjects showed with respect to target size. Moving forward, our next fMRI study would allow us to see the effects of changes in the stimuli design at the whole-brain level.

Looking to improve upon our first fMRI experimental design, several changes were made to our new imaging protocol to not only strengthen our first design but to investigate new ideas. In addition to a changed stimulus design, another area of task-design improvement included modulating the frequency of the active portion of the vergence-tracking task. The effect of modulating the frequency of the active portion of the vergence-tracking task was investigated where the active task was either coded to induce a slow or fast frequency of vergence movements. Smaller changes were incorporated as well: our voxel dimensions were reduced (3.0mm x 3.0mm x 3.0mm) where we were able to collect more brain slices.

As this project is a constituent of a broader, longitudinal NIH study investigating the sustained effect of vision therapy, achieving a high degree of reliability for our vergence-tracking task both within and between sessions is crucial in order to validate the potential effects of vergence therapy that subjects undergo. While the specific goal of the current fMRI study was to assess the reliability of a vergence-tracking task among controls, we sought to improve on our first fMRI experimental design by incorporating

several changes that were made to our imaging protocol to not only strengthen our first fMRI experimental design but to investigate new ideas as well.

With a multimodal approach that spanned the course of three specific projects, we were able to modify and strengthen experimental designs moving forward as our research findings and scientific investigation dictated. This dissertation began with an initial fMRI setup that consisted of LED targets positioned at locations along the subject's midline and a traditional 30s on/off vergence-tracking block design. By the final project, 3rd degree fusion stimuli were being programmatically controlled to follow a frequency modulated vergence-tracking protocol.

While the dissertation first began as a proof of concept, it has now surpassed the working concept stage into a reliable technical procedures document where the methodologies in all three projects have proven successful. It is my hope that this thesis dissertation can provide the groundwork for future fMRI studies in vergence tracking to build upon.

REFERENCES

Abrahamsson M, Ohlsson J, Björndahl M & Abrahamsson H. (2003). Clinical evaluation of an eccentric infrared photorefractor: The PowerRefractor. Acta Ophthalmologica Scandinavica, 81, 605–610.

Akao T, Kurkin SA, Fukushima J, Fukushima K. 2005. Visual and vergence eye movement-related responses of pursuit neurons in the caudal frontal eye fields to motion-in-depth stimuli. Exp Brain Res 164:92-108.

Alkan, Y., Biswal, B. B., & Alvarez, TL. (2011). Differentiation between Vergence and Saccadic Functional Activity within the Human Frontal Eye Fields and Midbrain Revealed through fMRI. PLoS ONE, 6, e25866.

Alkan, Y., Biswal, B. B., & Alvarez, TL. (2011). Differentiation between vergence and saccadic functional activity within the human frontal eye fields and midbrain revealed through fMRi. PLoS ONE, 6.

Alkan Y, Biswal BB, Taylor PA & Alvarez TL. (2011). Segregation of frontoparietal and cerebellar components within saccade and vergence networks using hierarchical independent component analysis of fMRI. Visual Neuroscience, 28, 247–261.

Alkan Y, Biswal BB, Alvarez TL. 2011. Differentiation between vergence and saccadic functional activity within the human frontal eye fields and midbrain revealed through fMRI. PLoS One.

Alkan Y, Biswal BB, Taylor PA, Alvarez TL. 2011. Segregation of frontoparietal and cerebellar components within saccade and vergence networks using hierarchical independent component analysis of fMRI. Visual Neuroscience 28.

Allen PM, Radhakrishnan H & O'Leary DJ. (2003). Repeatability and validity of the PowerRefractor and the Nidek AR600-A in an adult population with healthy eyes. Optometry and Vision Science : Official Publication of the American Academy of Optometry, 80, 245–251.

Alvarez TL, Alkan Y, Gohel S, Douglas Ward B, Biswal BB. 2010. Functional anatomy of predictive vergence and saccade eye movements in humans: a functional MRI investigation. Vision Res 50:2163-2175.

Alvarez, TL, Alkan, Y., Gohel, S., Douglas Ward, B., & Biswal, B. B. (2010). Functional anatomy of predictive vergence and saccade eye movements in humans: A functional MRI investigation. Vision Research, 50, 2163–2175.

Alvarez TL, Jaswal, R, Gohel, S., & Biswal, B. B. (2014). Functional activity within the frontal eye fields, posterior parietal cortex, and cerebellar vermis significantly correlates to symmetrical vergence peak velocity: an ROI-based, fMRI study of vergence training. Frontiers in Integrative Neuroscience, 8, 50.

Alvarez T. L., & Kim, E. H. (2013). Analysis of saccades and peak velocity to symmetrical convergence stimuli: Binocularly normal controls compared to convergence insufficiency patients. Investigative Ophthalmology and Visual Science, 54, 4122–4135.

Alvarez TL, Bhavsar M, Semmlow JL, Bergen MT, Pedrono C. 2005. Short-term predictive changes in the dynamics of disparity vergence eye movements. J Vis 5:640-649.

Alvarez TL, Semmlow JL, Yuan W, Munoz P. 2002. Comparison of Disparity Vergence System Responses to Predictable and Non-predictable Stimulations. Current Pscyhology of Cognition 21:243-261.

Alvarez TL, Vicci VR, Alkan Y, Kim EH, Gohel S, Barrett AM, Chiaravalloti N, Biswal BB. 2010. Vision therapy in adults with convergence insufficiency: clinical and functional magnetic resonance imaging measures. Optom Vis Sci 87:E985-1002.

Beckmann CF, Smith SM. 2004. Probabilistic independent component analysis for functional magnetic resonance imaging. IEEE Transactions on Medical Imaging 23:137-152.

Beckmann CF, Smith SM. 2005. Tensorial extensions of independent component analysis for multisubject FMRI analysis. NeuroImage 25:294-311.

Behzadi Y, Restom K, Liau J, Liu TT. 2007. A component based noise correction method (CompCor) for BOLD and perfusion based fMRI. Neuroimage 37:90-101.

Bharadwaj SR, Sravani NG, Little JA, Narasaiah A, Wong V, Woodburn R, & Candy T R. (2013). Empirical variability in the calibration of slope-based eccentric photorefraction. Journal of the Optical Society of America. A, Optics, Image Science, and Vision, 30, 923–31.

Biswal B, Yetkin FZ, Haughton VM, Hyde JS. 1995. Functional connectivity in the motor cortex of resting human brain using echo-planar MRI. Magn Reson Med 34:537-541.

Biswal BB, Mennes M, Zuo XN, Gohel S, Kelly C, Smith SM, Beckmann CF, Adelstein JS, Buckner RL, Colcombe S, Dogonowski AM, Ernst M, Fair D, Hampson M, Hoptman MJ, Hyde JS, Kiviniemi VJ, Kotter R, Li SJ, Lin CP, Lowe MJ, Mackay C, Madden DJ, Madsen KH, Margulies DS, Mayberg HS, McMahon K, Monk CS, Mostofsky SH, Nagel BJ, Pekar JJ, Peltier SJ, Petersen SE, Riedl V, Rombouts SA, Rypma B, Schlaggar BL, Schmidt S, Seidler RD, Siegle GJ, Sorg C, Teng GJ, Veijola J, Villringer A, Walter M, Wang L, Weng XC, Whitfield-Gabrieli S, Williamson P, Windischberger C, Zang YF, Zhang HY, Castellanos FX, Milham MP. 2010. Toward discovery science of human brain function. Proceedings of the National Academy of Sciences of the United States of America 107:4734-4739.

Blade PJ, & Candy TR. (2006). Validation of the PowerRefractor for measuring human infant refraction. Optometry and Vision Science : Official Publication of the American Academy of Optometry, 83, 346–353.

Blautzik J, Keeser D, Berman A, Paolini M, Kirsch V, Mueller S, Coates U, Reiser M, Teipel SJ, Meindl T. 2012. Long-Term Test-Retest Reliability of Resting-State Networks in Healthy Elderly Subjects and Mild Cognitive Impairment Patients. J Alzheimers Dis. 2013;34(3):741-54.

Brannen JH, Badie B, Moritz CH, Quigley M, Meyerand ME, Haughton VM. 2001. Reliability of functional MR imaging with word-generation tasks for mapping Broca's area. AJNR Am J Neuroradiol. 2001 Oct;22(9):1711-8.

Breveglieri R, Hadjidimitrakis K, Bosco A, Sabatini SP, Galletti C, Fattori P. 2012. Eye position encoding in three-dimensional space: integration of version and vergence signals in the medial posterior parietal cortex. J Neurosci 32:159-169.

Carvelho T, Allison RS, Irving EL & Herriot C. (2008). Computer gaming for vision therapy. In 2008 Virtual Rehabilitation, IWVR (pp. 198–204).

Chen Y-F, Lee YY, Chen T, Semmlow JL, Alvarez TL. 2010. Behaviors, Models and Clinical Applications of Vergence Eye Movements. Journal of Medical and Biological Engineering 3:1-15.

Choi M, Weiss S, Schaeffel F, Seidemann A, Howland HC, Wilhelm B & Wilhelm H. (2000). Laboratory, clinical, and kindergarten test of a new eccentric infrared photorefractor (PowerRefractor). Optometry and Vision Science: Official Publication of the American Academy of Optometry, 77, 537–548.

Chui TYP, Song H, Clark CA, Papay JA, Burns SA & Elsner AE. (2012). Cone photoreceptor packing density and the outer nuclear layer thickness in healthy subjects. Investigative Ophthalmology and Visual Science, 53, 3545–3553.

Cicerone CM, & Nerger JL. (1989). The relative numbers of long-wavelength-sensitive to middle-wavelength-sensitive cones in the human fovea centralis. Vision Research, 29, 115–128.

Collewijn, H. & Erkelens, C. J.in Eye Movements and their Role in Visual and Cognitive Processes(ed. Kowler, E.) 213–261 (Elsevier, Amsterdam, (1990).

Convergence Insufficiency Treatment Trial (CITT) Study Group. The convergence insufficiency treatment trial: design, methods, and baseline data. Ophthalmic Epidemiol. 2008 Jan-Feb;15(1):24-36.

Convergence Insufficiency Treatment Trial (CITT) Study Group. Long-term effectiveness of treatments for symptomatic convergence insufficiency in children. Optom Vis Sci. 2009 Sep;86(9):1096-103.

Cooper J, Jamal N. 2012. Convergence insufficiency-a major review. Optometry 83:137-158.

Cooper JS, Burns CR, Cotter SA, Daum KM, Griffin JR, Scheiman MM. 2011. Care of the Patient with Accommodative and Vergence Dysfunction. In. American Optometric Association. St. Louis: American Optometric Association.

Coubard OA, Kapoula Z. 2008. Saccades during symmetrical vergence. Graefe's archive for clinical and experimental ophthalmology = Albrecht von Graefes Archiv fur klinische und experimentelle Ophthalmologie 246:521-536.

Cox RW. 1996. AFNI: software for analysis and visualization of functional magnetic resonance neuroimages. Computers and biomedical research, an international journal 29:162-173.

Ciuffreda, K. J., Rutner, D., Kapoor, N., Suchoff, I. B., Craig, S., & Han, M. E. (2008). Vision therapy for oculomotor dysfunctions in acquired brain injury: A retrospective analysis. Optometry, 79, 18–22.

Daum KM. 1984. Convergence insufficiency. Am J Optom Physiol Opt 61:16-22.

Faul, F, Erdfelder E, Lang, AG, & Buchner, A. (2007). G*Power 3: A flexible statistical power analysis program for the social, behavioral, and biomedical sciences. Behavior Research Methods, 39, 175-191.

Ferraina S, Brunamonti E, Giusti MA, Costa S, Genovesio A, Caminiti R. 2009. Reaching in depth: hand position dominates over binocular eye position in the rostral superior parietal lobule. J Neurosci 29:11461-11470.

Ferraina S, Pare M, Wurtz RH. 2000. Disparity sensitivity of frontal eye field neurons. J Neurophysiol 83:625-629.

Fogt N, Jones R. Comparison of the monocular occlusion and a direct method for objective measurement of fixation disparity. Optom Vis Sci. 1997; 74:43-50.

Freyer T, Valerius G, Kuelz AK, Speck O, Glauche V, Hull M, Voderholzer U. 2009. Test-retest reliability of event-related functional MRI in a probabilistic reversal learning task. Psychiatry research 174:40-46.

Fukushima K, Yamanobe T, Shinmei Y, Fukushima J, Kurkin S, Peterson BW. 2002. Coding of smooth eye movements in three-dimensional space by frontal cortex. Nature 419:157-162.

Gamlin PD. 2002. Neural mechanisms for the control of vergence eye movements. Ann N Y Acad Sci 956:264-272.

Gamlin PD, Yoon K. 2000. An area for vergence eye movement in primate frontal cortex. Nature 407:1003-1007.

Gamlin PD, Yoon K, Zhang H. 1996. The role of cerebro-ponto-cerebellar pathways in the control of vergence eye movements. Eye (Lond) 10 (Pt 2):167-171.

Genovesio A, Ferraina S. 2004. Integration of retinal disparity and fixation-distance related signals toward an egocentric coding of distance in the posterior parietal cortex of primates. J Neurophysiol 91:2670-2684.

Geschwind N. 1970. The organization of language and the brain. Science 170:940-944.

Gnadt JW, Mays LE. 1995. Neurons in monkey parietal area LIP are tuned for eye-movement parameters in three-dimensional space. J Neurophysiol 73:280-297.

Golestani AM, Tymchuk S, Demchuk A, Goodyear BG. 2013. Longitudinal evaluation of resting-state FMRI after acute stroke with hemiparesis. Neurorehabil Neural Repair 27:153-163.

Gowdy PD & Cicerone CM. (1998). The spatial arrangement of the L and M cones in the central fovea of the living human eye. Vision Research, 38, 2575–2589.

Griffin JR. 1988. Binocular Anomalies Procedures For Vision Therapy. New York, NY: Professional Press Books Fairchild Publications.

Grisham JD. 1988. Visual therapy results for convergence insufficiency: a literature review. Am J Optom Physiol Opt 65:448-454.

Hillemanns M. (1927). Die funktionelle Asymmetrie der Augen, die Vorherrschaft eines derselben und die binokulare Richtungsloka- lisation. Klinische Monatsblatter Fur Augenheilkunde, 78, 737–761.

Horng JL, Semmlow JL, Hung GK & Ciuffreda KJ. (1998). Dynamic asymmetries in disparity convergence eye movements. Vision Research, 38(18), 2761–8.

Horwood AM, Riddell PM. A novel experimental method for measuring vergence and accommodation responses to the main near visual cues in typical and atyipical groups. Strabismus. 2009; 17:9-15.

Howard IP, Rogers BJ. Seeing Depth. 2nd ed. Toronto: I. Porteous, 2002.

Hughes A., AC/A ratio, Br J Ophthalmol, vol. 51, pp. 78607, Nov 1967.

Hung G & Huston R. (2002). Models of Oculomotor Control. Applied Mechanics Reviews.

Hung GK, Semmlow JL & Ciuffreda KJ. (1986). A dual-mode dynamic model of the vergence eye movement system. IEEE Transactions on Bio-Medical Engineering, 33, 1021–1028.

Hunt, O. A., Wolffsohn, J. S., & Gilmartin, B. (2003). Evaluation of the measurement of refractive error by the PowerRefractor: a remote, continuous and binocular measurement system of oculomotor function. The British Journal of Ophthalmology, 87, 1504–1508.

Hutchison RM, Gallivan JP, Culham JC, Gati JS, Menon RS, Everling S. 2012. Functional connectivity of the frontal eye fields in humans and macaque monkeys investigated with resting-state fMRI. J Neurophysiol 107:2463-2474.

Jenkinson M, Bannister P, Brady M, Smith S. 2002. Improved optimization for the robust and accurate linear registration and motion correction of brain images. NeuroImage 17:825-841.

Jenkinson M, Smith S. 2001. A global optimisation method for robust affine registration of brain images. Medical Image Analysis 5:143-156.

Judge SJ.in Vision and Visual Dysfunction, 8: Eye Movements (ed. Carpenter, R. H. S.) 157–172 (Macmillan, London, (1991).

Judge SJ. Vergence. In: Carpenter RHS, ed. Eye Movements. London: Macmillan Press, 1991:157-174.

Kapoula Z, Isotalo E, Muri RM, Bucci MP, Rivaud-Pechoux S. 2001. Effects of transcranial magnetic stimulation of the posterior parietal cortex on saccades and vergence. Neuroreport 12:4041-4046.

Kapoula Z, Yang Q, Coubard O, Daunys G, Orssaud C. 2004. Transcranial magnetic stimulation of the posterior parietal cortex delays the latency of both isolated and combined vergence-saccade movements in humans. Neurosci Lett 360:95-99.

Kapoula Z, Yang Q, Coubard O, Daunys G, Orssaud C. 2005. Role of the posterior parietal cortex in the initiation of saccades and vergence: right/left functional asymmetry. Ann N Y Acad Sci 1039:184-197.

Khosroyani, M., & Hung, G. K. (2002). A dual-mode dynamic model of the human accommodation system. Bulletin of Mathematical Biology, 64, 285–299.

Kiehl KA, Liddle PF. (2003). Reproducibility of the hemodynamic response to auditory oddball stimuli: a six-week test-retest study. Hum Brain Mapp 18:42-52.

Kim, EH, & Alvarez, TL. (2012). The frequency of horizontal saccades in near and far symmetrical disparity vergence. Vision Research, 63, 9–19.

Kim E, & Alvarez TL. (2011). The frequency of saccades correlates to peak velocity in symmetrical disparity vergence. In Proceedings of the Annual International Conference of the IEEE Engineering in Medicine and Biology Society, EMBS (pp. 1664–1667).

Kim KH, Relkin NR, Lee KM, Hirsch J. 1997. Distinct cortical areas associated with native and second languages. Nature 388:171-174.

Kim SG, Ogawa S. 2012. Biophysical and physiological origins of blood oxygenation level-dependent fMRI signals. Journal of cerebral blood flow and metabolism: official journal of the International Society of Cerebral Blood Flow and Metabolism 32:1188-1206.

Kimmig H, Greenlee MW, Gondan M, Schira M, Kassubek J, & Mergner T. (2001). Relationship between saccadic eye movements and cortical activity as measured by fMRI: Quantitative and qualitative aspects. Experimental Brain Research, 141, 184–194.

Kotulak JC and Schor CM. The dissociability of accommodation from vergence in the dark. Invest Ophthalmol Vis Sci, vol. 27, pp. 544-51, Apr 1986.

Krauskopf J. (2000). Relative number of long- and middle-wavelength-sensitive cones in the human fovea. Journal of the Optical Society of America. A, Optics, Image Science, and Vision, 17, 510–516.

Kumar AN, Han Y, Garbutt S, Leigh RJ. 2002. Properties of anticipatory vergence responses. Invest Ophthalmol Vis Sci 43:2626-2632.

Kumar AN, Han Y, Ramat S, Leigh RJ. 2002. Anticipatory saccadic-vergence responses in humans. Ann N Y Acad Sci 956:495-498.

Laatsch L, Krisky C. 2006. Changes in fMRI activation following rehabilitation of reading and visual processing deficits in subjects with traumatic brain injury. Brain Inj 20:1367-1375.

Laatsch LK, Thulborn KR, Krisky CM, Shobat DM, Sweeney JA. 2004. Investigating the neurobiological basis of cognitive rehabilitation therapy with fMRI. Brain Inj 18:957-974.

Leavitt VM, Wylie GR, Girgis PA, Deluca J, Chiaravalloti ND. 2012. Increased functional connectivity within memory networks following memory rehabilitation in multiple sclerosis. Brain Imaging Behav.

Lombardo M, Serrao S, Ducoli P, & Lombardo G. (2013a). Eccentricity dependent changes of density, spacing and packing arrangement of parafoveal cones. Ophthalmic and Physiological Optics, 33, 516–526.

Lombardo, M., Serrao, S., Ducoli, P., & Lombardo, G. (2013b). Influence of sampling window size and orientation on parafoveal cone packing density. Biomedical Optics Express, 4, 1318–31.

Loubinoux I, Carel C, Alary F, Boulanouar K, Viallard G, Manelfe C, Rascol O, Celsis P, Chollet F. 2001. Within-session and between-session reproducibility of cerebral sensorimotor activation: a test--retest effect evidenced with functional magnetic resonance imaging. J Cereb Blood Flow Metab 21:592-607.

Lukasova K, Sommer J, Nucci-da-Silva MP, Vieira G, Blanke M, Bremmer F, Sato JR, Kircher T, Amaro E, Jr. 2013. Test-retest reliability of fMRI activation generated by different saccade tasks. J Magn Reson Imaging.

Lund TE, Norgaard MD, Rostrup E, Rowe JB, Paulson OB. 2005. Motion or activity: their role in intra- and inter-subject variation in fMRI. Neuroimage 26:960-964.

Maddox EE. The Clinical Use of Prisms: And the Decentering of Lenses. 2nd edition. Bristol, England: John Wright & Sons, 1893.

Margulies DS, Bottger J, Long X, Lv Y, Kelly C, Schafer A, Goldhahn D, Abbushi A, Milham MP, Lohmann G, Villringer A. 2010. Resting developments: a review of fMRI post-processing methodologies for spontaneous brain activity. Magma 23:289-307.

Maruta J, Ghajar J. Detecting eye movement abnormalities from concussion. Prog Neurol Surg. 2014;28:226-33.

Meindl T, Teipel S, Elmouden R, Mueller S, Koch W, Dietrich O, Coates U, Reiser M, Glaser C. 2010. Test-retest reproducibility of the default-mode network in healthy individuals. Hum Brain Mapp 31:237-246.

Ming J, Thulborn KR, Szlyk JP. 2012. Reproducibility of activation maps for longitudinal studies of visual function by functional magnetic resonance imaging. Invest Ophthalmol Vis Sci 53:6153-6163.

Nakamura T, Hillary FG, Biswal BB. 2009. Resting network plasticity following brain injury. PLoS One 4:e8220.

Nguyen D, Vedamurthy I, Schor C. Cross-coupling between accommodation and convergence is optimized for a broad range of directions and distances of gaze. Vision Res. 2008; 48:893-903.

Nitta T, Akao T, Kurkin S, Fukushima K. 2008. Involvement of the cerebellar dorsal vermis in vergence eye movements in monkeys. Cereb Cortex 18:1042-1057.

Nitta T, Akao T, Kurkin S, Fukushima K. 2008. Vergence eye movement signals in the cerebellar dorsal vermis. Prog Brain Res 171:173-176.

Optican, L. M. (2010). Oculomotor System: Models. In Encyclopedia of Neuroscience (pp. 25–34).

Parisi L, Rocca MA, Mattioli F, Copetti M, Capra R, Valsasina P, Stampatori C, Filippi M. 2013. Changes of brain resting state functional connectivity predict the persistence of cognitive rehabilitation effects in patients with multiple sclerosis. Mult Scler.

Park CH, Chang WH, Ohn SH, Kim ST, Bang OY, Pascual-Leone A, Kim YH. 2011. Longitudinal changes of resting-state functional connectivity during motor recovery after stroke. Stroke; a journal of cerebral circulation 42:1357-1362.

Park, S. P., Chung, J. K., Greenstein, V., Tsang, S. H., & Chang, S. (2013). A study of factors affecting the human cone photoreceptor density measured by adaptive optics scanning laser ophthalmoscope. Experimental Eye Research, 108, 1–9.

Peelen MV, Downing PE. 2005. Within-subject reproducibility of category-specific visual activation with functional MRI. Hum Brain Mapp 25:402-408.

Pickwell LD, Hampshire R. 1981. The significance of inadequate convergence. Ophthalmic Physiol Opt 1:13-18.

Prevosto V, Graf W, Ugolini G. 2010. Cerebellar inputs to intraparietal cortex areas LIP and MIP: functional frameworks for adaptive control of eye movements, reaching, and arm/eye/head movement coordination. Cereb Cortex 20:214-228.

Quinlan DJ, Culham JC. 2007. fMRI reveals a preference for near viewing in the human parieto-occipital cortex. Neuroimage 36:167-187.

Rashbass, C. & Westheimer, G. Disjunctive eye movements. J. Physiol. (Lond.) 159, 339–360

Raemaekers M, Bergsma DP, van Wezel RJ, van der Wildt GJ, van den Berg AV. 2011. Effects of vision restoration training on early visual cortex in patients with cerebral blindness investigated with functional magnetic resonance imaging. J Neurophysiol 105:872-882.

Roper-Hall G. Historical bignette: Ernest Edmund Maddox (1860-1933): master surgeon, inventor, and investigator. Am Orthopt J. 2009; 59:103-110.

Rouse MW, Borsting EJ, Mitchell GL, Scheiman M, Cotter SA, Cooper J, Kulp MT, London R, Wensveen J. 2004. Validity and reliability of the revised convergence insufficiency symptom survey in adults. Ophthalmic Physiol Opt 24:384-390.

Rosenbach, O. (1903). Über monokulare Vorherrschaft beim binokularen Sehen. Münch. Med. Wochenschr, 30, 1290–1292.

Sakata H, Taira M, Kusunoki M, Murata A, Tsutsui K, Tanaka Y, Shein WN, Miyashita Y. 1999. Neural representation of three-dimensional features of manipulation objects with stereopsis. Exp Brain Res 128:160-169.

Sander T, Sprenger A, Neumann G, Machner B, Gottschalk S, Rambold H, Helmchen C. 2009. Vergence deficits in patients with cerebellar lesions. Brain 132:103-115.

Satterthwaite TD, Elliott MA, Gerraty RT, Ruparel K, Loughead J, Calkins ME, Eickhoff SB, Hakonarson H, Gur RC, Gur RE, Wolf DH. 2013. An improved framework for confound regression and filtering for control of motion artifact in the preprocessing of resting-state functional connectivity data. Neuroimage 64:240-256.

Scheiman M, Gwiazda J, Li T. 2011. Non-surgical interventions for convergence insufficiency. Cochrane Database Syst Rev 3:CD006768.

Scheiman M, Rouse M, Kulp MT, Cotter S, Hertle R, Mitchell GL. 2009. Treatment of convergence insufficiency in childhood: a current perspective. Optom Vis Sci 86:420-428.

Scheiman M, Wick B. 2008. Binocular Vision Heterophoric, Accommodative and Eye Movement Disorders: Lippincott Williams & Wilkins.

Scheiman M, Mitchell GL, Cotter S, Kulp MT, Cooper J, Rouse M, Wensveen J. (2005). A randomized clinical trial of vision therapy/orthoptics versus pencil pushups for the treatment of convergence insufficiency in young adults. Optometry and vision science : official publication of the American Academy of Optometry (Vol. 82, pp. 583–595).

Semmlow JL, Chen Y-F, Granger-Donetti B, Alvarez TL. 2009. Correction of Saccade-Induced Midline Errors in Responses to Pure Disparity Vergence Stimuli. J Eye Movement Res 2:1-13.

Semmlow JL, Chen Y-F, Pedrono C, Alvarez TL. 2008. Saccadic Behavior during the Response to Pure Disparity Vergence Stimuli I: General Properties. J Eye Movement Res 1:1-11.

Shainberg, M. J. (2010). Vision therapy and orthoptics. American Orthoptic Journal, 60, 28–32.

Shaywitz SE, Shaywitz BA, Fulbright RK, Skudlarski P, Mencl WE, Constable RT, Pugh KR, Holahan JM, Marchione KE, Fletcher JM, Lyon GR, Gore JC. 2003. Neural systems for compensation and persistence: young adult outcome of childhood reading disability. Biological psychiatry 54:25-33.

Shehzad Z, Kelly AM, Reiss PT, Gee DG, Gotimer K, Uddin LQ, Lee SH, Margulies DS, Roy AK, Biswal BB, Petkova E, Castellanos FX, Milham MP. 2009. The resting brain: unconstrained yet reliable. Cereb Cortex 19:2209-2229.

Shin HS, Park SC, & Maples, W. C. (2011). Effectiveness of vision therapy for convergence dysfunctions and long-term stability after vision therapy. Ophthalmic and Physiological Optics, 31, 180–189.

Smith SM. 2002. Fast robust automated brain extraction. Human brain mapping 17:143-155.

Song J, Desphande AS, Meier TB, Tudorascu DL, Vergun S, Nair VA, Biswal BB, Meyerand ME, Birn RM, Bellec P, Prabhakaran V. 2012. Age-related differences in test-retest reliability in resting-state brain functional connectivity. PLoS One 7:e49847.

Song H, Chui TYP, Zhong Z, Elsner AE & Burns SA. (2011). Variation of cone photoreceptor packing density with retinal eccentricity and age. Investigative Ophthalmology and Visual Science, 52, 7376–7384.

Specht K, Willmes K, Shah NJ, Jancke L. 2003. Assessment of reliability in functional imaging studies. J Magn Reson Imaging 17:463-471.

Sravani NG, Nilagiri VK, Bharadwaj SR. Photorefraction estimates of refractive power varies with the ethnic origin of human eyes. Sci Rep. 2015 Jan 23;5:7976.

Stark L, Kenyon RV, Krishnan VV et al. Disparity vergence: a proposed name for a dominant component of binocular vergence eye mvoements. Am J Optom Phyiol Opt. 1980: 57:606-609.

Stone J, Pal S, Blackburn D, Reuber M, Thekkumpurath P, Carson A. Functional (Psychogenic) Cognitive Disorders: A Perspective from the Neurology Clinic. J Alzheimers Dis. 2015 Sep 24;48 Suppl 1:S5-S17.

Taira M, Tsutsui KI, Jiang M, Yara K, Sakata H. 2000. Parietal neurons represent surface orientation from the gradient of binocular disparity. J Neurophysiol 83:3140-3146.

Taubert M, Lohmann G, Margulies DS, Villringer A, Ragert P. 2011. Long-term effects of motor training on resting-state networks and underlying brain structure. Neuroimage 57:1492-1498.

Tseng P, Chang CF, Chiau HY, Liang WK, Liu CL, Hsu TY, Hung DL, Tzeng OJ, Juan CH. 2013. The dorsal attentional system in oculomotor learning of predictive information. Frontiers in Human Neuroscience 7:404.

Tyler CW, Likova LT, Mineff KN, Nicholas SC. Deficits in the activation of human oculomotor nuclei in chronic traumatic brain injury. Front Neurol. 2015 Aug 25;6:173.

Van Horn MR, Waitzaman DM, Cullen KE. Vergence neurons identified in the rostral superior colliculus code smooth eye movements in 3D space. J Neurosci. 2013 Apr 24;33(17):7274-84.

Ventura RE, Balcer LJ, Galetta SL, Rucker JC. (2016). Ocular motor assessment in concussion: Current status and future directions. J Neurol Sci. 2016 Feb 15;361:79-86.

Von Noorden GK, Campos EC. 2002. Binocular vision and ocular motility: Theory and management of strabismus. St. Louis, MI: Mosby.

Walls GL. (1951). A theory of ocular dominance. Archives of Ophthalmology, 45, 387–412.

Yang Q, Kapoula Z. 2004. TMS over the left posterior parietal cortex prolongs latency of contralateral saccades and convergence. Invest Ophthalmol Vis Sci 45:2231-2239.

Yetkin FZ, McAuliffe TL, Cox R, Haughton VM. 1996. Test-retest precision of functional MR in sensory and motor task activation. AJNR Am J Neuroradiol 17:95-98.

Yoo SS, Wei X, Dickey CC, Guttmann CR, Panych LP. 2005. Long-term reproducibility analysis of fMRI using hand motor task. The International journal of neuroscience 115:55-77.

Zhang Y, Brady M, Smith S. 2001. Segmentation of brain MR images through a hidden Markov random field model and the expectation-maximization algorithm. IEEE transactions on medical imaging 20:45-57.

Zhu DC, Covassin T, Nogle S, Doyle S, Russell D, Pearson RL, Monroe J, Liszewski CM, DeMarco JK, Kaufman DI. A potential biomarker in sports-related concussion: brain functional connectivity alteration of the default-mode network measured with longitudinal resting-state fMRI over thirty days. J Neurotrauma. 2015 Mar 1;32(5):327-41.

Zou KH, Greve DN, Wang M, Pieper SD, Warfield SK, White NS, Manandhar S, Brown GG, Vangel MG, Kikinis R, Wells WM, 3rd. 2005. Reproducibility of functional MR imaging: preliminary results of prospective multi-institutional study performed by Biomedical Informatics Research Network. Radiology 237:781-789.

APPENDIX A

CLINICAL PARAMETERS

Figure A.1 – A.3 shows all clinical parameters collected.

					NPC			NPA
Subject ID	Age	Gender	OS Rx	OD Rx	Blur	Break	Recovery	Blur
1	19	f	-0.5	-0.25	12	5	11	10
2	20	m	-4	-4	16	5	8	6
3	21	m	-2.5	-2.75	x	3	4	9
4	18	m	-5.25	-5.25	12	5	11	x
5	22	f	0.25	0.25	8	6	9	6
6	33	m	-3.75	-4.75	7	5	7	8
7	30	m	x	x	x	8	5	x
8	18	f	20/20	20/20	10	3	12	7
9	18	f	20/20	20/20	9	3	9	5
10	21	f	-3.25	-3.25	9	6	10	x
11	22	f	20/20	20/20	9	5	8	x
12	20	m	-2.25	-2.25	10	7	9	6
13	22	m	x	x	x	2.5	4	7
14	25	m	-0.75	-1	0	5	6	x
15	19	m	-3.25	-3.5	9	3	10	6
16	27	m	-5	-5	0	4	6	x
17	23	m	-1.25	-1	13	9	13	X
18	22	f	-0.5	-0.5	8	2	8	5

Figure A.1

	Stereopsis		Vergence Range					
Subject ID	Local	Global Randot	Base Out			Base In		
1	40	250	x	x	x	x	x	x
2	20	250	20	20	18	12	12	10
3	20	250	25	45	40	x	12	10
4	20	250	x	20	18	16	30	20
5	20	250	x	45+	45+	Na	18	14
6	30	250	20	30	25	12	14	12
7	30	250	x	x	x	x	x	x
8	30	250	x	14	10	14	35	30
9	20	250	30	40	35	x	18	16
10	70	250	25	45	40	x	x	x
11	50	250	x	x	x	x	x	x
12	20	250	x	18	10	x	14	12
13	20	250	16	20	18	x	25	20
14	30	250	25	40	35	x	x	x
15	30	250	20	30	25	16	20	18
16	30	250	x	16	14	x	18	12
17	40	250	x	35	30	x	20	18
18	20	250	18	25	20	x	x	x

Figure A.1

	Vergence Facility		Motor and Sensory Preference					
Subject ID	Flips/min	Trouble w/	Motor Near	Motor Far	Sensory Near RG	Sensory Far RG	Sensory Near GR	Sensory Far GR
1	x	x	R	R	M	R	G	G
2	45	none	L	R	G	G	M	R
3	17	base in	R	L	R	G	R	G
4	x	x	R	L	M	R	G	R
5	56	none	L	L	M	M	G	G
6	36	none	R	R	R	R	M	M
7	x	x	R	L	R	M	R	M
8	53	none	L	L	M	W	G	G
9	30	none	L	L	M	M	M	M
10	19	base in	R	R	G	M	G	M
11	42	none	R	R	G	M	R	M
12	50	none	L	R	G	G	G	G
13	27	base in	R	R	R	R	R	R
14			R	R	M	M	M	M
15	22	none	R	R	M	M	M	M
16			R	R	R	M	M	M
17	20	base in	L	L	G	L	M	M
18	31	none	L	L	G	G	G	M

Figure A.3